

REFERENCES

1. Paris, L. and Cortina, R.,  
"Switching and lightning impulse discharge characteristics of large air gaps and long insulator strings", IEEE Trans., Vol. PAS 87, No. 4, April 1968, pp 947-957.
2. Glavitsch, H.,  
"Problems associated with switching surges in e.h.v. networks", Brown Boveri Review, Vol.53, No. 4/5, April/May 1966, pp 267-277.
3. Köppl, G. and Ruoss, E.,  
"Switching overvoltages in e.h.v. and u.h.v. networks", Brown Boveri Review, No. 12, 1970, pp 554-561.
4. Baltensperger, P. and Ruoss, E.,  
"Switching overvoltages in e.h.v. and u.h.v. networks", CIGRE Report No. 13-14, 1970, pp 1-13.
5. Thoren, H.B.,  
"Reduction of switching overvoltages in e.h.v. and u.h.v. systems", IEEE Trans., Vol. PAS 90, 1971, pp 1321-1326.
6. Yeckley, R.N., Friedrich, R.E. and Thuot, M.E.,  
"E.h.v. breaker rated for control of closing voltage switching surges to 1.5 per unit", IEEE Trans., Vol. PAS 91, mar/Apr 1972, pp 399-403.
7. Schei, A. and Johansson, A.,  
"Temporary overvoltages and protective requirements for e.h.v. and u.h.v. arrestors", CIGRE Report No. 33-04, 1972, pp 1-14.
8. Thoren, H.B. and Carlsson, K.L.,  
"A digital computer program for the calculation of switching and lightning surges on power systems", IEEE Trans., Vol. PAS 89, No.2, February 1970, pp 212-218.

9. Ozay, N.,  
"Analysis of energisation transients of transmission lines",  
Ph.D. Thesis, UMIST, 1970.
10. Abetti, P.A.,  
"Transformer models for the determination of transient  
voltages", AIEE Trans., Vol.72, Part III, June 1953, pp 468-480.
11. Abetti, P.A. and Davis H.F.,  
"Surge transfer in three-winding transformers", AIEE Trans.,  
Part III, December 1954, pp 1395-1407.
12. Abetti, P.A.,  
"Electrostatic voltage distribution and transfer in three-  
winding transformers", AIEE Trans., Part III, December 1954,  
pp 1407-1416.
13. Brown, J.I., Morsztyn, K. and Wright, I.A.,  
"A new transient analyser", Paper No.2746, I.E.Australia,  
October 1968, pp 3-10.
14. Clerici, A. and Taschini, A.,  
"Influence on switching surges of the switched zero sequence  
impedance", IEEE Trans., Vol. PAS 90, 1971, pp 1327-1333.
15. Merry, S.M. and Taylor, E.R.,  
"Overvoltages and harmonics on e.h.v. systems", IEEE  
Trans., Vol. PAS 89, No. 5/6, May/June 1970, pp 685-690.
16. Wilson, D.D.,  
"Phase-phase switching surges on 500-kV transformer terminated  
lines, Part I : 500-kV circuit breaker operation", IEEE  
Trans., Vol. PAS 89, No. 5/6, May/June 1970, pp 685-690.
17. Wilson D.D.,  
"Phase-phase switching surges on 500-kV transformer terminated

lines, Part II : Switching from low-voltage terminals",  
IEEE Trans., Vol. PAS 89, No. 5/6, May/June 1970, pp 691-697.

18. White, E.L.,  
"Surge-transference characteristics of generator-transformer installations", Proc. IEE, Vol. 116, No. 4, April 1959, pp 575-587.
19. Heller, B. and Veverka, A.,  
"Surge phenomena in electrical machines", (Book) Translation by Vosper J.S., London Iliffe Books Ltd., 1968.
20. Gururaj, B.L.,  
"Natural frequencies of 3-phase transformer windings", IEEE Trans., Vol. PAS 82, June 1963, pp 318-329.
21. Johansen, I.,  
"Natural frequencies in power-transformer windings", AIEE Trans., Vol. 78, June 1959, pp 129,136.
22. White, E.L.,  
"An experimental study of surges and oscillations in windings of core-type transformers", Proc. IEE, Vol. 107, Part A, 1960, pp 421-431.
23. Hileman, A.R.,  
"Surge transfer through three-phase transformers", AIEE Trans., Part III, February 1959, pp 1543-1554.
24. White, E.L.,  
"Controlled current chopping as a possible overvoltage test method for transformers on site", ERA Report No. 5134, 1965.
25. Bewley, L.V.,  
"Equivalent circuits of transformers and reactors to switching surges", AIEE Trans., Vol. 58, 1939, pp 797-802.
26. Arlette, P.L. and Murray-Shelley, R.,  
"The teaching of travelling wave techniques using an improved

- graphical method - I", IJEEE, Vol.4, 1966, pp 213-230.
27. Arlette, P.L., and Murray-Shelley, R.,  
"The teaching of travelling wave techniques using an improved graphical method - II", IJEEE, Vol. 4, 1966, pp 327-349.
  28. Bickford, J.P.,  
"Calculation of switching transients with particular reference to line energisation", Proc. IEE, Vol. 114, No.4, April, 1967, pp 465-477.
  29. Battisson, M.J., Bickford, J.P., Corcoran, J.C.W., Jackson, R.L., Scott, M. and Ward, R.J.S.,  
"British investigations on the switching of long e.h.v. transmission lines", CIGRE, 1970, Report No. 13-02.
  30. Bolton, E., Battisson, M.J., Bickford, J.P., Dwek, M.G., Jackson, R.L. and Scott, M.,  
"Short-line fault tests on the CEGB 275 kV system", Proc. IEE, Vol. 117, No.4, April 1970, pp 771-784.
  31. Danh, M.D.N.,  
"Transient performance of cross-bonded cable systems", Ph.D. Thesis, UMIST, July 1972.
  32. Selvavinayamoorthy, S.,  
"Evaluation of overvoltages in power system networks due to surge phenomena", Ph.D. Thesis, UMIST, October 1973.
  33. Lucas, J.R.,  
"Cross-bonded cables and analysis of non-linearities", M.Sc. dissertation, UMIST, October 1972.
  34. Day, S.J., Mullineux, N. and Reed, J.R.,  
"Developments in obtaining transient response using Fourier integrals : Part I - Gibbs oscillation and Fourier integrals", IJEEE, Vol. 3, 1965, pp 501-506.

35. Day, S.J., Mullineux, N. and Reed, J.R.,  
"Developments in obtaining transient response using Fourier integrals : Part II - Use of the modified Fourier transform", IJEEE, Vol. 4, 1966, pp 31-40.
36. Battisson, M.J., Day, S.J., Mullineux, N. and Reed, J.R.,  
"Developments in obtaining transient response using Fourier integrals: Part III - Global response", IJEEE, Vol. 6, 1968, pp 259-265.
37. Cooley, J.W.,  
"Applications of the fast Fourier transform method", Proc. IBM Scientific Computing Symp., June 1966.
38. Ametani, A.,  
"Application of the fast Fourier transform to electrical transient phenomena", IJEEE, No. 4, Vol. 10, 1972.
39. Hedman, D.E.,  
"Theoretical evaluation of multiphase propagation", IEEE Trans., Vol. PAS 90, No. 3, 1971, pp 1312-1320.
40. Dommel, H.W.,  
"Digital computer solution of electromagnetic transients in single- and multi-phase networks", IEEE Trans., Vol. PAS 88, No. 4, April 1969, pp 388-399.
41. Heaton, A.G. and Reid, I.A.,  
"Transient overvoltages and power-line terminations", Proc. IEE, Vol. 113, No. 3, March 1966, pp 461-470.
42. Rau, N.S. and Janischewskyj, W.,  
"A numerical method for the calculation of transients in linear and non-linear transmission lines - State equations approach", IEEE Trans., Vol. PAS 91, 1972, pp 2545-2552.
43. Wedepohl, L.M.,  
"Application of matrix methods to the solution of travelling wave phenomena in polyphase systems", Proc. IEE, Vol. 110, No. 12, 1963, pp 2200 - 2212.

44. Wedepohl, L.M. and Mohamed, S.E.T.,  
"Multiconductor transmission lines. Theory of natural modes and Fourier integrals applied to transient analysis", Proc. IEE, Vol.116, 1969, pp 1553-1563.
45. Kuo, F.F.,  
"Network analysis and synthesis", John Wiley and Sons, Tokyo, (Book), 1966, Second Edition.
46. Kron, G.,  
"Tensor analysis of networks", MacDonald & Co., Publishers, Ltd., London, (Book), 1964.
47. Li, K.K.,  
"The parameters of transformer windings for surge distribution calculations", M.Sc. dissertation, UMIST, 1971.
48. Morstyn, K. and Wilson, A.,  
"Laboratory investigation of core flux pattern in cold and hot rolled steel transformers during impulse testing", IJEEE, Vol. 6, pp 375-387.
49. Pireme, J.,  
"Fondements d'une nouvelle theorie et synthese des theories actuelles : Premiere partie", Revue Generale de l'Electricite, Vol. 47, No. 1-2, pp 20-32.
50. Carson, J.R.,  
"Wave propagation in overhead wires with ground return", Bell Syst. Tech. J., 1926, Vol.5, pp 539-554.
51. Dwek, M.G., Hall, J.E., Jackson, R.L. and Jones, B.,  
"Field tests and analysis to determine switching transients on the British system", CIGRE Report No.13-03, pp1-18.
52. McElroy, A.J., Price, W.S., Smith, H.M. and Shankle, D.F.,  
"Field measurements of switching surges on unterminated 345 kV transmission lines", AIEE.Trans., Aug. 1963, pp 465-487.

53. Price, W.S., McElroy, A.J., Smith, H.M. and Shankle, D.F.,  
"Field measurements of 345 kV lightning arrester switching surge performance", AIEE Trans., Aug 1963, pp 487-500.
54. McElroy, A.J., Price, W.S., Smith, H.M. and Shankle, D.F.,  
"Field measurements of switching surges as modified by unloaded 345 kV transformers", AIEE Trans., Aug 1963, pp 500-520.
55. Alexander, G.W., Mielke, J.E. and Trojan, H.T.,  
"Switching surges on Northern States power company's 345 kV circuits", IEEE Trans., Vol PAS-88, No. 6, June 1969, pp 919-931.
56. I E E E Committee Report,  
"Switching surges: II - Selection of typical waves for insulation co-ordination", IEEE Trans., Vol PAS-85, Oct 1966, pp 1091-1097.
57. I E E E Committee Report,  
"Switching surges, part III: Field and analyser results for transmission lines - past, present, and future trends", IEEE trans., Vol PAS-89, No. 2, Feb 1970, pp 173-189.
58. Committee Report,  
"Switching surge field tests on the Arizona Public Service 345 kV system", IEEE Trans, Vol PAS-87, No.7, July 1968, pp 1635-1648.
59. Csuros, L. and Foreman, K.F.,  
"Energising overvoltages on transformer-feeder circuits",  
Electrical Times, 31 August 1972, pp 37-40.
60. Csuros, L., Foreman, K.F. and Glavitsch, H.,  
"Energising overvoltages on transformer feeders", Electra,  
No.18, pp 83-105



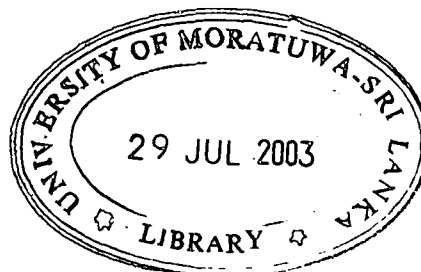
61. Swift, G.W.,  
"Power transformer core behaviour under transient conditions",  
IEEE Trans, PAS 90, Jan-Feb 1971, pp 2206-2210.
62. Sarbach, E.,  
"Limitation of switching surges by arresters and the effect  
of network parameters on arrester stresses", Brown Boveri  
Review, April/May 1966, pp 291-297.
63. Breuer, G.D., Csuros, L., Flugum, R.W., Kauferle, J. and Schei, A.,  
"H.V.D.C. surge divertors and their application for overvoltage  
protection of H.V.D.C. schemes", CIGRE Report No. 33-14, 1972.
64. Phelps, J.D.M. and Flugum, R.W.,  
"New concepts in the application of surge arresters for  
insulation co-ordination", CIGRE Report No. 33-08, 1972, pp 1-11.
65. Beavers, M.F., Holcomb, J.E. and Leoni, L.C.,  
"Magnetization of transformer cores during impulse testing",  
AIEE Trans., Vol 74, Part III, April 1955, pp 118-124.
66. Algrbrant, A., Brierley, A.E., Hylten-Cavallius, N., and Ryder, D.H.,  
"Switching surge testing of transformers", IEEE Trans.,  
Vol PAS 85, No.1, Jan 1966, pp 54-61.
67. Nakra, H.L. and Barton, T.H.,  
"The dynamics of coupled circuits with ferromagnetic non-  
linearity", IEEE Trans., 1972, pp 2349-2358.
68. Macfadyen, W.K., Simpson, R.R.S., Slater, R.D. and Wood, W.S.,  
"Method of predicting transient-current patterns in transformers",  
Proc. IEE, Vol 120, No. 11, Nov 1973, pp 1393-1396.
69. Mullineux, N. and Reed, J.R.,  
"Developments in obtaining transient response using Fourier  
transforms : Part IV - Survey of the theory", I.J.E.E.E.,  
1972, pp 256-267.



70. Ganz, A.G.,  
"Leakage inductance and equivalent networks of transformers",  
IEEE Trans., Parts, Materials & Packaging, PMP 4, No 3,  
Sept 1968, pp 67-68.
71. Galloway, R.H., Shorrocks, W.B. and Wedepohl, L.M.,  
"Calculation of electrical parameters for short and long  
polyphase transmission lines", Proc. IEE, Vol 111, No. 12,  
pp 2051-2059.
72. Wilcox, D.J.,  
"Transients and harmonic induction in underground cable systems",  
Ph.D. Thesis, UMIST, 1969.
73. Wedepohl, L.M. and Mohamed, S.E.T.,  
"Transient analysis of multiconductor transmission lines with  
special reference to nonlinear problems", Proc. IEE, Vol 117,  
No. 5, May 1970, pp 979-988.



University of Moratuwa, Sri Lanka  
Electronic Theses & Dissertations  
[www.lib.mrt.ac.lk](http://www.lib.mrt.ac.lk)



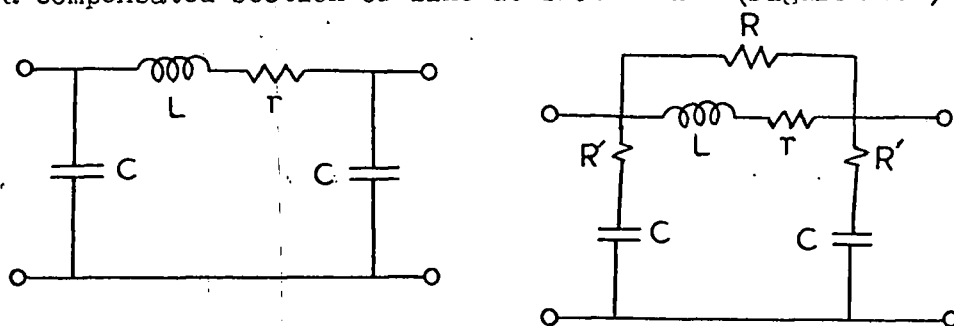
APPENDIX 1METHODS OF ANALYSISA1.1 Transient Network Analyser

The calculation of transients in power systems have traditionally been carried out using transient network analysis (TNA) on suitable models. Transmission lines are represented by a finite number of lumped element ladder networks to simulate the distributed parameters of the line. Additional passive elements are used to represent the network devices such as transformers, loads, source impedance, lightning arrestors so that a complete analogue of the system is obtained. The main advantage of the TNA are its flexibility and the ability to produce instantaneous results for a variety of system studies. In the transient analysers, to reduce the size of capacitors and inductors used in the system, time scaling factors are quite often used.

Transformers may be included in the system as scaled models of convenient size. Geometric<sup>10</sup>, equivalent circuit and electro-magnetic<sup>12</sup> models have all been used in the past, but they suffer from the inherent problem that all relevant parameters cannot be simultaneously scaled.

In a recent study<sup>13</sup>, use is made of a near ideal transformer with completely linear characteristic, with non-linearities such as due to the magnetising characteristic being electronically simulated in the analogue system, so that any type of core material may be represented.

Since the transmission line is represented by a finite number of sections, an upper limit is placed on the frequency response determined by the natural frequency of an individual section. Thus spurious oscillations occur which have a frequency corresponding to the product of the number of sections and the line fundamental frequency. However, this spurious oscillations may be suppressed by using a compensated section of line as shown below (Figure A1.1)<sup>29</sup>.



Section-Uncompensated Model Line      Section-Compensated Model Line

Figure A1.1

University of Moratuwa, Sri Lanka.  
Electronic Theses & Dissertations  
www.lib.mrt.ac.lk

The earth return path is usually represented by an earth-branch inductance and resistance. Figure A1.2 shows a single section of a three-phase model compensated line with earth return path.

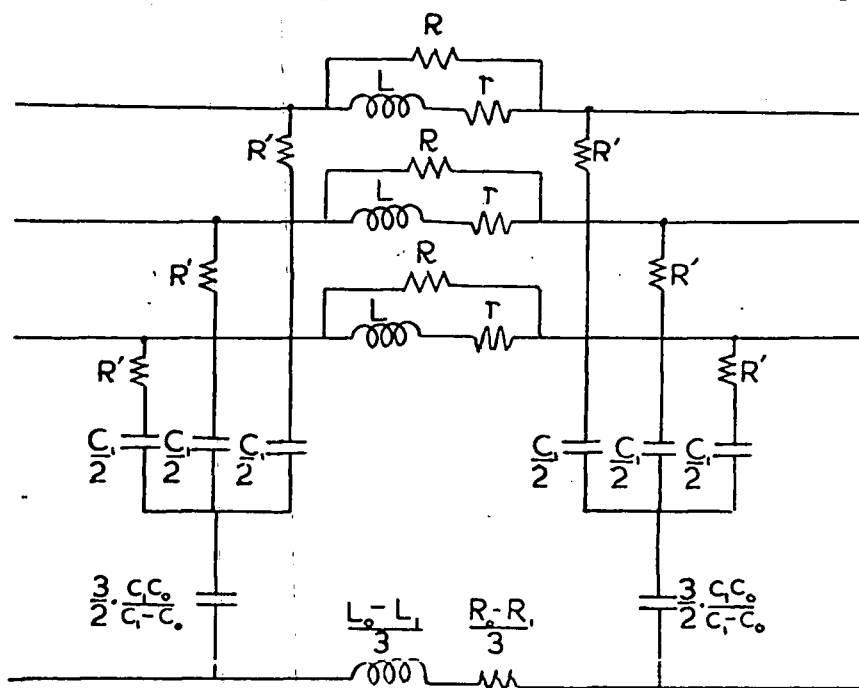
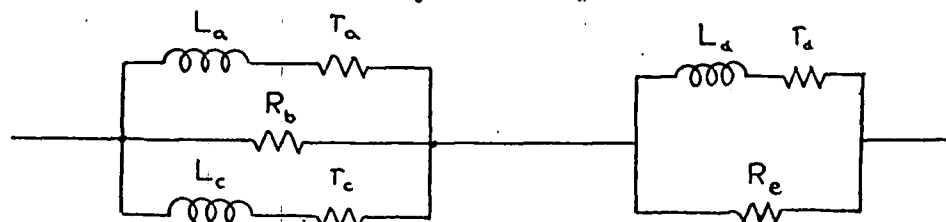


Figure A1.2 Three-phase Compensated Model Line

More sophisticated representation using additional inductances and resistances can be used to correctly represent the frequency characteristic for earth return path<sup>14</sup>. Figure below shows the sophisticated earth-branch representation. However, for normal calculations this is not really necessary.



( $r_a, r_c$  and  $r_d$  are resistances inherent in the inductors  $L_a, L_c$  and  $L_d$ )

Figure A1.3 Sophisticated Earth-Branch Representation

A repetition rate is chosen so that a steady oscilloscope display is obtained while allowing sufficient time for the decay of transients from previous switching operations. Mercury-wetted relays are used to simulate Circuit breaker operation. The point-on-wave operation of each switch can be controlled independently<sup>13</sup>. The controls of the switches can also be inter-linked so as to simulate resistor insertion by each pole of a three-pole circuit breaker. The point-on-wave of operation can then be scanned automatically through the power frequency cycle.

Alternatively, a more sophisticated technique is for the analyser to be controlled by a small digital computer and the system can be programmed to perform Monte-Carlo testing to determine an over-voltage probability distribution. Using the facilities of the hybrid system a number of studies can be performed which would otherwise be impractical because of the large number of random switching operations required.

### A1.2 Lattice Diagram Method

The general solution to the transmission line equations may be expressed as the sum of forward and reverse travelling wave functions as

$$V = \underbrace{F_f\left(t - \frac{x}{v}\right)}_{\substack{\text{forward} \\ \text{wave}}} + \underbrace{F_r\left(t + \frac{x}{v}\right)}_{\substack{\text{reverse} \\ \text{wave}}}$$

where  $F_f$  and  $F_r$  are arbitrary functions of space  $x$  and time  $t$  chosen to suit initial conditions.

This travelling wave equation has been used in a graphical solution by Bewley<sup>25</sup>. The method known as the Lattice diagram technique treats all lines as being basically lossless. This method has been extended by Bickford<sup>28</sup> and others for use on the digital computer, the lattice diagram itself being replaced by a 'Branch Timetable'. In the method, all circuit elements are represented by transmission lines with distributed parameters. A basic time interval is chosen for each transient calculation and has a value less than the travel of the shortest line to be represented. All lines are then expressed as integral multiples of the basic time interval as corresponding to their time of travel. Lumped values of inductances and capacitances representing transformers, generators, series and shunt compensation, stray capacitances etc., are replaced by 'transmission line stubs' by defining the surge impedance  $Z$  of the 'stub' in terms of its inductance or capacitance, and an arbitrarily chosen small time constant  $\tau$ .

$$Z = \sqrt{\frac{L}{C}}, \quad \tau = \sqrt{LC}$$

where  $L$  and  $C$  are the inductance and capacitance of the 'stub' line.

An inductor is represented by a stub line with surge impedance given by  $Z = L/\tau_L$  and travel time  $\tau_L$ , while a capacitance is represented by a stub line with surge impedance  $Z = \tau_C/C$  and travel time  $\tau_C$ . It is generally satisfactory to choose this travel time as equal to or half the basic time interval depending on connection of lumped element. In general it is found necessary to ensure that the surge impedance of inductive and capacitive stubs are respectively greater than ten times and less than one tenth the combined equivalent surge impedance of all other circuits connected to the same busbar.

The waveforms of voltage and currents applied to the system are synthesised by the use of step functions which travel along the line. Their behaviour at the junctions and terminations is determined by reflection and transmission coefficients.

Consider the junction J between two impedances  $Z_1$  and  $Z_2$  as shown in figure A1.4 below, and let unit voltage arrive along  $Z_1$  to the junction J

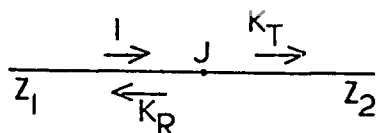


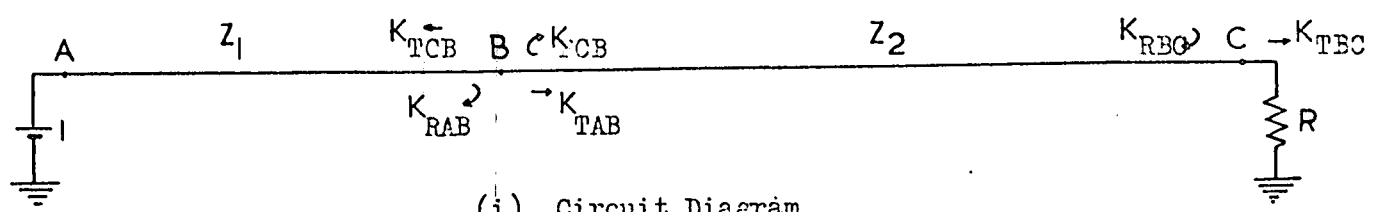
Figure A1.4

If  $K_R$  and  $K_T$  are the reflection and transmission coefficients, then it can be shown that these are given by the expressions

$$K_R = \frac{Z_2 - Z_1}{Z_2 + Z_1}, \quad K_T = \frac{2 Z_2}{Z_2 + Z_1} = 1 + K_R$$

Figure A1.5 shows the application of the technique to transmission lines in series, with a load resistor  $R$  at one end and fed by an infinite source at the other end.

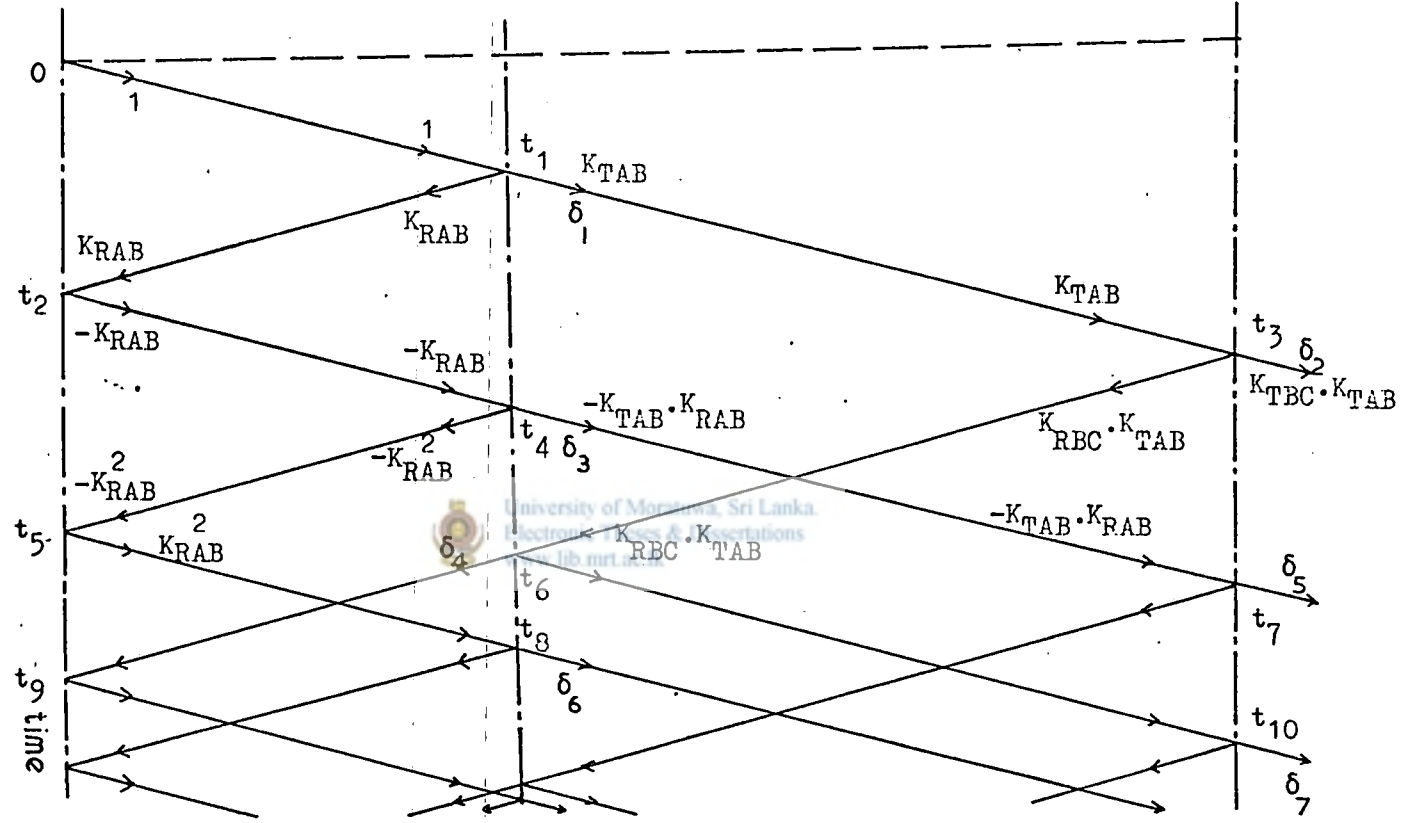
For the three-phase calculations, the above coefficients are replaced by the reflection and transmission matrices, and the mutual effects are thus included. However, the frequency dependence of line parameters cannot be taken into account and the parameters are



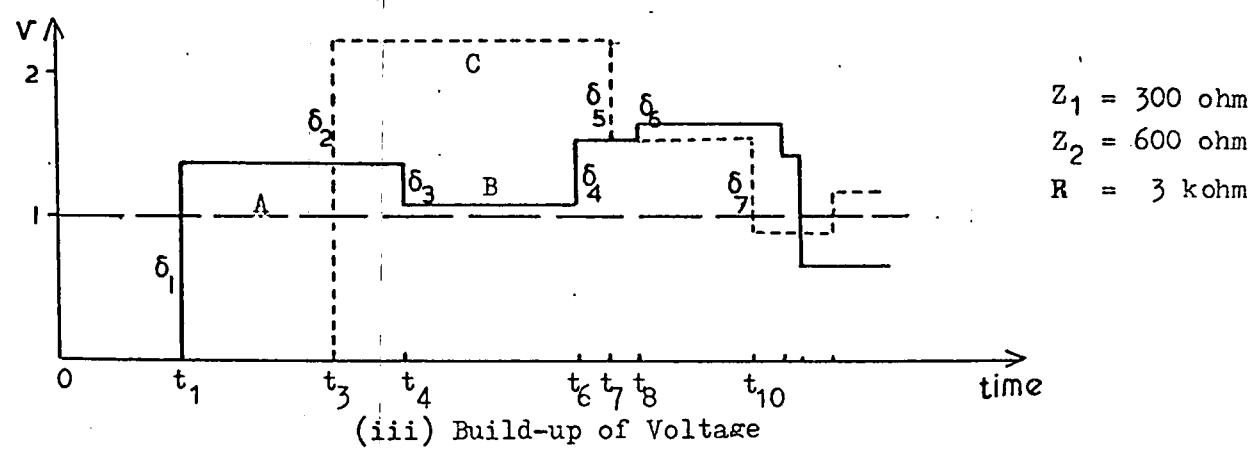
(i) Circuit Diagram

$$K_{RAB} = \frac{Z_2 - Z_1}{Z_2 + Z_1}, \quad K_{RBC} = \frac{R - Z_2}{R + Z_2}, \quad K_{RCB} = \frac{Z_1 - Z_2}{Z_1 + Z_2}$$

$$K_{TAB} = \frac{2 Z_2}{Z_2 + Z_1}, \quad K_{TBC} = \frac{2 R}{R + Z_2}, \quad K_{TCB} = \frac{2 Z_1}{Z_1 + Z_2}$$



(ii) Lattice Diagram



(iii) Build-up of Voltage

Figure A1.5 Application of Lattice Diagram Technique

generally calculated at a predominant frequency, if this is known, or on a frequency based on the travel time of the line under consideration. It is possible to partially account for the frequency dependence of the line parameters and of the losses, by transforming all voltage steps entering a line into the natural modes of propagation, where they may be suitably attenuated and distorted before being transformed back into phase quantities when they arrive at an end of the line. (This attenuation and distortion is generally done by pre-determining the response of the line to a unit step using Fourier analysis). Volt-ampere nonlinearities at the terminals may be accommodated in the calculations. However, three-phase transformers where interphase mutual coupling exists are not easily taken into account, as representation of lumped parameter elements by transmission line stubs proves rather cumbersome.



### A1.3 Schnyder-Bergeron Method

In the Schnyder-Bergeron method the transmission line problem is primarily solved on the volt-ampere co-ordinate axes using the travelling wave phenomena. The lines are represented by their surge impedances and travel times. Voltage sources and resistors are represented on the diagram by their volt-ampere characteristics.

The solution of the transmission line equation may be expressed in the travelling wave form as<sup>26,27</sup>

$$v = \underset{\substack{\text{forward} \\ \text{wave}}}{F_f(x - at)} + \underset{\substack{\text{reverse} \\ \text{wave}}}{F_r(x + at)} \quad (a)$$

$$\text{and } i = \frac{1}{Z} F_f(x - at) - F_r(x + at) \quad (b)$$



where

- a = velocity of wave propagation
- t = instant of time
- x = instantaneous position of wave
- Z = surge impedance of line

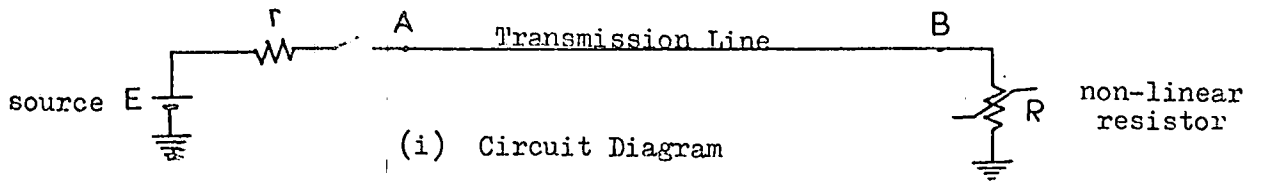
From equations (a) and (b),

$$v + Z i = 2 F_f(x - at)$$

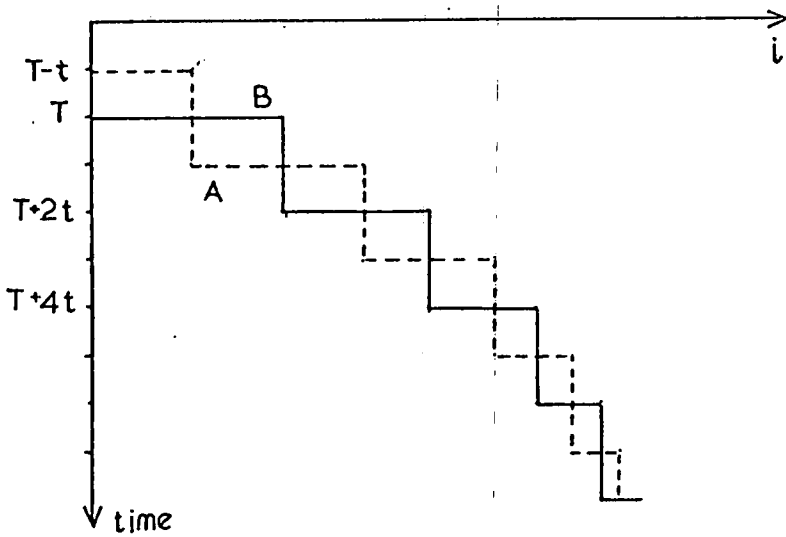
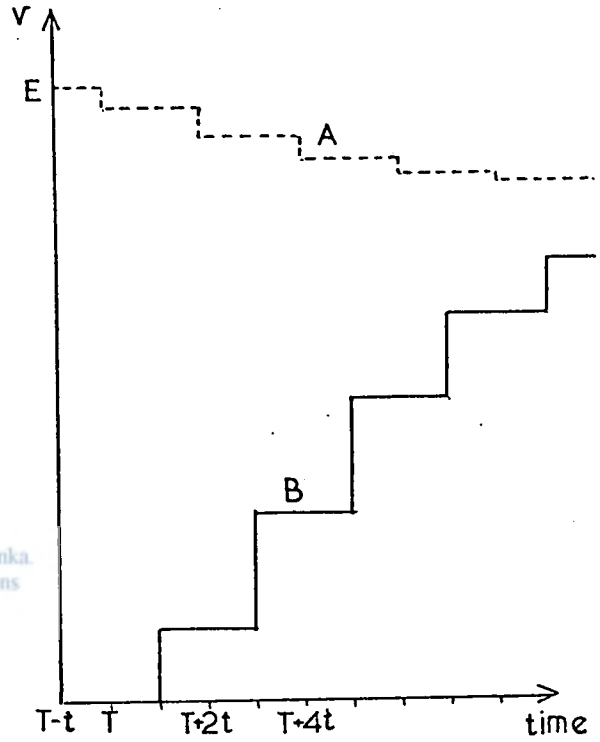
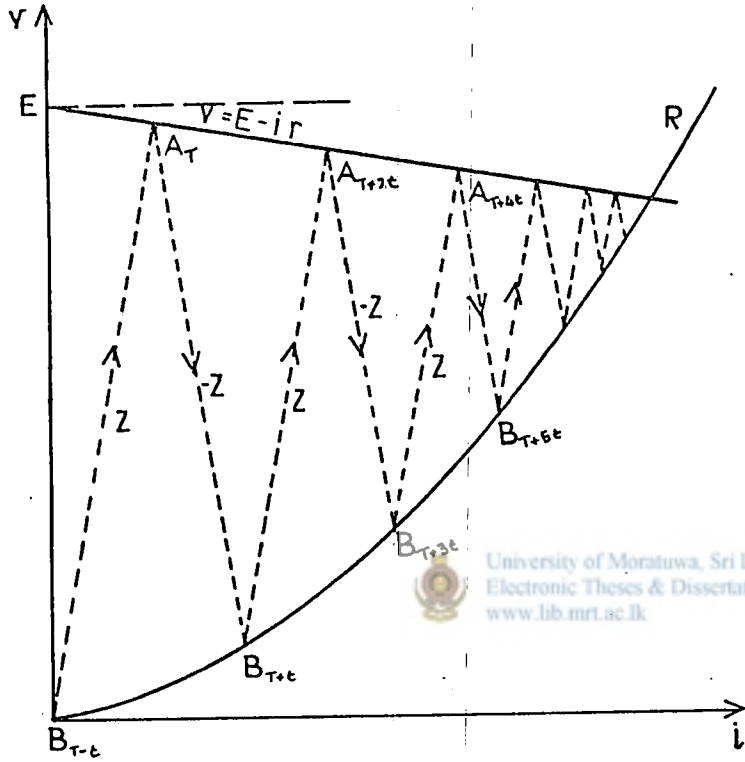
$$v - Z i = 2 F_r(x + at)$$

If, in these equations the factors  $(x-at)$  and  $(x+at)$  respectively are made constant, then the left hand side of the equations,  $v+Zi$  and  $v-Zi$  also become constant. The method of solution is based on this observation. The forward and reverse travelling waves are represented by line segments with positive and negative slopes respectively, and magnitudes of the transmitted voltage and current increments are obtained from intersections on the characteristics.. The increments are summed and plotted against the corresponding times to give the required waveforms. FigureA1.6 overleaf shows the application of the technique to a transmission line supplied by a voltage source with a finite internal impedance, loaded at the far end by a non linear load R. The figure also shows how the voltage and the current waveforms are simultaneously obtained from the volt-ampere diagram.

As in the lattice diagram method, lumped values of inductances and capacitances are represented by transmission line 'stubs', based on a chosen 'basic time interval'.



T - time at which time closes  
 t - travel time of line  
 Z - surge impedance of line  
 r - internal impedance of line



(ii) Build-up of Voltage and Current Waves

Figure A1.6 Application of the Bergeron Technique

This method too has been recently extended for use on the digital computer. The initial conditions define the voltages existing at all named busbars. Surge propagation is initiated by connecting the source system to the circuit to be energised. The program computes the voltage and current at each discrete point for each basic time interval. Multi-conductor representation is achieved using modal propagation techniques, the modal components being transformed into phase quantities at named busbars. Transmission parameters are chosen at a single frequency usually based on line length. Attenuation factors are included approximately by introducing series resistance into the modal domain.

An advantage of the method is that system non-linearities may be handled relatively easily without being involved in many mathematical equations. Another advantage of the method is that both voltage and current are always considered so that the current does not require a separate calculation. However, in handling lumped elements which are reactive in nature, a certain amount of approximation is necessary, so that if mutual coupling between phases in a transformer are to be considered, the problem tends to become excessively complex.

#### A1.4 Direct Integration Technique (State Space Formulation)

The method is based on the solution of a system of first order differential equations. In this method the transmission line length is divided into a suitable number of equal intervals or is represented by a laddered form of network. If the ladder approximation to the transmission line is used, the circuit (including representation

of terminal equipment) may be expressed in the form of a first order differential equation. Or, if the more accurate transmission line representation is used, finite difference formulae are used to obtain an ordinary differential equation approximation to the partial differential equations of the line. Whichever method is used, the ordinary differential equations can be reduced to the form<sup>41,42</sup>

$$\dot{x} = A x + B v$$

where

$x$  = vector of unknown voltages and currents

$\dot{x}$  = time derivative of vector  $x$

$A, B$  = matrices built from transmission line parameters

$v$  = vector of input forcing functions.

When dealing with transmission line parameters, the  $A$  and  $B$  matrices are re-evaluated at each stage of calculation.

When the system of ordinary differential equations is linear with constant coefficients, a closed form of solution is possible. The method then provides not only the overall transient response, but also the separate contributions of the various equivalent-circuit modes. The closed solution is based on the eigen values and modal matrix of matrix  $A$ . The transform of unknown voltages and currents is then obtained as a direct function of the transform of the forcing function, the modal matrix, the eigenvalues and the initial conditions. Inverse transformation then gives the unknown variables.

When non-linear parameters are present the method just described cannot be applied as the forcing functions need updating. In this case, the matrix ordinary differential equation is solved

using a numerical integration technique such as the fourth order Runge-Kutta method. In the method the response of the line (voltages and currents) are computed at all the discretized points along the line and terminal equipment. The method can be easily adopted to solve non-linear boundary value problems.

However, the differential equations for the ladder approximation to a transmission line are computationally in attractive due to the high value of the spectral radius (high frequencies of oscillation) of the resulting equations.

#### A1.5 Modified Fourier Transform <sup>69</sup>

The major problem with the previous methods described in this Appendix has been one of adequate simulation of the transmission line distortion and attenuation because of the deficiency in representing the frequency dependant parameters of the line and earth. Another of the problems was the complete representation of the coupling of flux in a transformer.

In the Fourier transform method, the transient problem is analysed by transforming the applied wave into its frequency components. The transform  $F(w)$  of a forcing function  $f(t)$  is given by<sup>34</sup>

$$F(w) = \int_0^{\infty} f(t) \cdot e^{-j w t} dt$$

If  $H(w)$  is the transform of the transfer function of a network, then the transform of the response,  $R(w)$ , is given by

$$R(w) = H(w) \cdot F(w)$$

and the response,  $r(t)$ , in the time domain is given by

$$r(t) = \frac{2}{\pi} \int_0^{\infty} R(\omega) \cdot e^{j\omega t} d\omega$$

However, with a practical network, it is generally not possible to obtain the inverse transform analytically, and the numerical form of the integral is used for purposes of computation. Thus

$$r(t) = \frac{2}{\pi} \sum_0^{\Omega} R(\omega) \cdot e^{j\omega t} \cdot \Delta\omega$$

where

$\Delta\omega$  = chosen frequency step length for numerical integration

$\Omega$  = maximum value of the angular frequency considered.

Limiting the maximum frequency to a finite value gives rise to an oscillation known as Gibb's phenomenon, while the finite frequency step length gives rise to a limit on the maximum attainable rise time of the waveform. The Gibb's oscillation is generally reduced<sup>34</sup> by using a suitable sigma factor ( $\sigma$ )

$$\sigma = \frac{\text{Sin}(\omega/\Omega)\pi}{(\omega/\Omega)\pi}$$

The sigma factor has an effect of reducing the rise time slightly, in addition to reducing the Gibb's oscillation.

Fourier analysis has the advantage that differential equations are simplified into ordinary equations. Also, the application of the method to the calculation of switching transients is attractive because, as shown by Carson<sup>50</sup>, the mutual coupling, distortion and attenuation of travelling waves on transmission lines are frequency dependant. These phenomena can be very conveniently catered for during the calculation of the frequency response, since at each stage

the relevant value of line impedance can be used.

In Fourier analysis, the transform function may have poles along the real frequency axis, and would cause instability when obtaining the inverse transform. Thus, in the modified Fourier transform, a shift factor  $\alpha$  is introduced so as to shift the line of integration away from the real frequency axis. This shift has the effect of decaying the forcing function by a factor  $e^{-\alpha t}$ , obtaining the response in the usual way and then pre-multiplying the response thus obtained by  $e^{\alpha t}$  to obtain the actual waveform. In this case the parameters are calculated at a complex frequency given by<sup>35</sup>

$$w = w_{\text{real}} - j\alpha$$

where  $w_{\text{real}}$  is the real component of the frequency. When transforming back to the time domain, the inverse transform process is generally quite cumbersome especially when dealing with a large number of frequency steps. Fortunately, there is a certain repetitiveness in this inversion process, which when properly utilised, tremendously reduces the amount of computation required. However, a slight amount of additional storage is required for the organised process of inversion. This method, known as the Fast Fourier technique has been used in certain sections of the present work to cut down the computation cost. However, when sequential switching operations are considered, unlike in the normal inversion process, the complete inversion would have to be repeated for each of the times at which switching occurs, so that the technique loses some of its advantage.

In the general method of analysis, modal components are used in the calculation of two-port admittance parameters for the transmission

lines. Matrix equations are easily formed using the usual nodal analysis. The problem is solved in the frequency plane and then transformed into the time domain, to give the desired voltage and current waveforms. A complete representation of the transformer including interphase mutual coupling and frequency dependant losses is easily achieved in the analysis.





APPENDIX 2ANALYSIS OF SWITCHING SURGES BY FOURIER TRANSFORMA2.1 Introduction

In the present work, the analysis of the transient problem is carried out in the frequency domain using the Modified Fourier Transform (Appendix A1.5). In this, the numerical process used for the inverse transform requires an upper limit to be placed on the frequency spectrum of the waveform and a finite step length to be chosen for the numerical integration. Thus, in order to obtain the overvoltages caused by the switching operations, it is necessary to investigate the range of frequencies to be considered, and the parameters involved.

The following sections describe the various factors that need to be considered, and the problems that may be encountered.

A2.2 Sigma Factor <sup>35</sup>

Figures A2.1 and A2.2 show typical forms of switching surges which are analysed using the Fourier transform. The figures also show that a large amount of Gibb's oscillation occurs when the inversion integral is evaluated numerically, due to the upper limit on the frequency. However, as shown in figure A2.3, the use of a 'sigma factor' (to be defined later) reduces the Gibb's oscillation to negligible proportions. It is also seen that there is a slight loss in the initial rate of rise.

As the mathematical analysis of these waveforms is quite complex, investigations are based on the unit step function. This wave

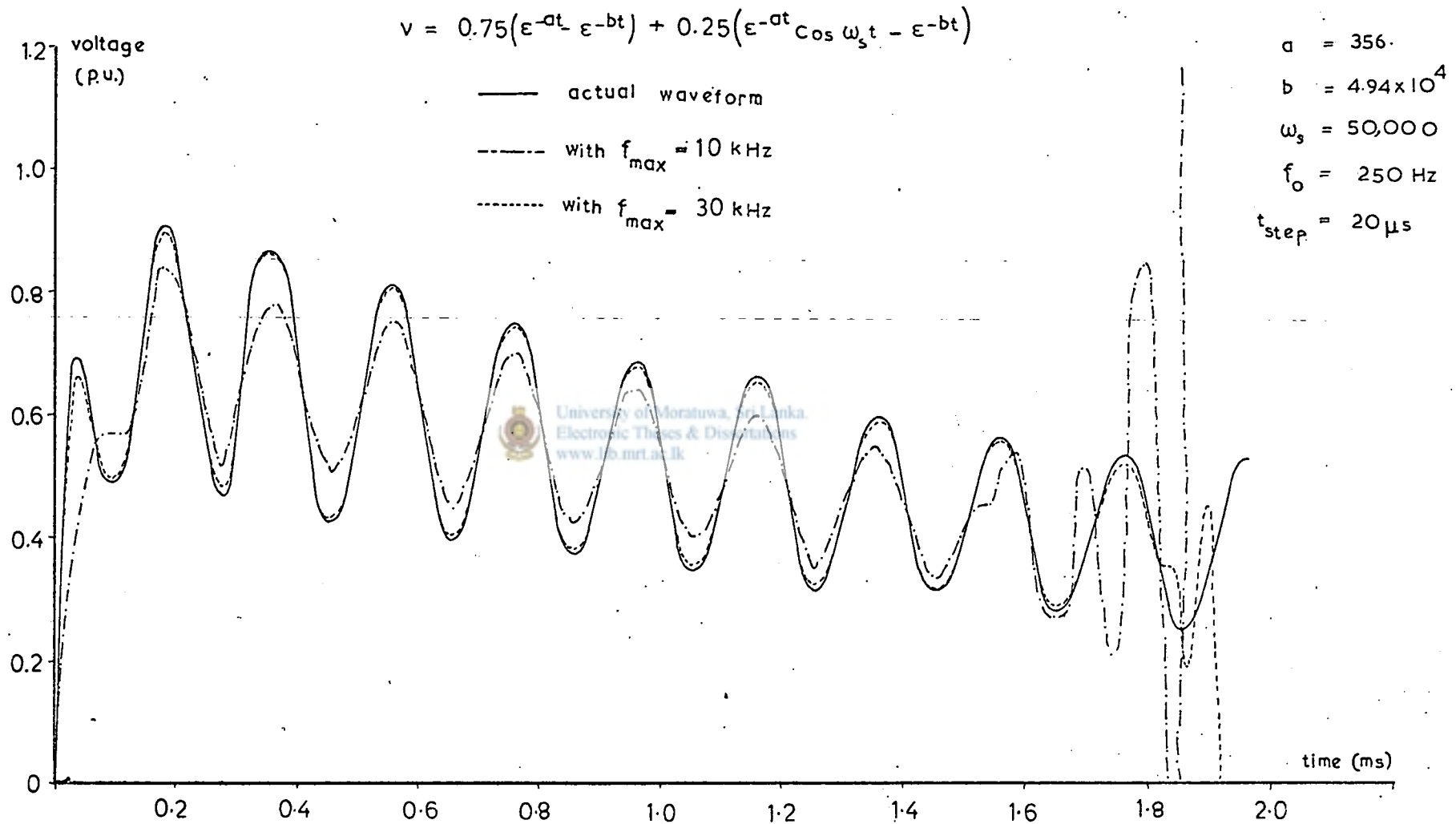


Figure A2.1 Effect of Increasing frequency - range

$$v = \cos \omega_s t - \frac{2}{3} \cos \omega_1 t - \frac{1}{3} \cos \omega_2 t$$

$$\begin{aligned} \omega_s &= 100\pi \\ \omega_1 &= 2400\pi \\ \omega_2 &= 3200\pi \\ \omega_o &= 50\pi \\ \Delta t &= 50\mu s \end{aligned}$$

- 1 - actual waveform
- 2 - with  $\omega_m = 3000\pi$
- 3 - "  $\omega_m = 6000\pi$
- 4 - "  $\omega_m = 9000\pi$
- 5 - "  $\omega_m = 12000\pi$

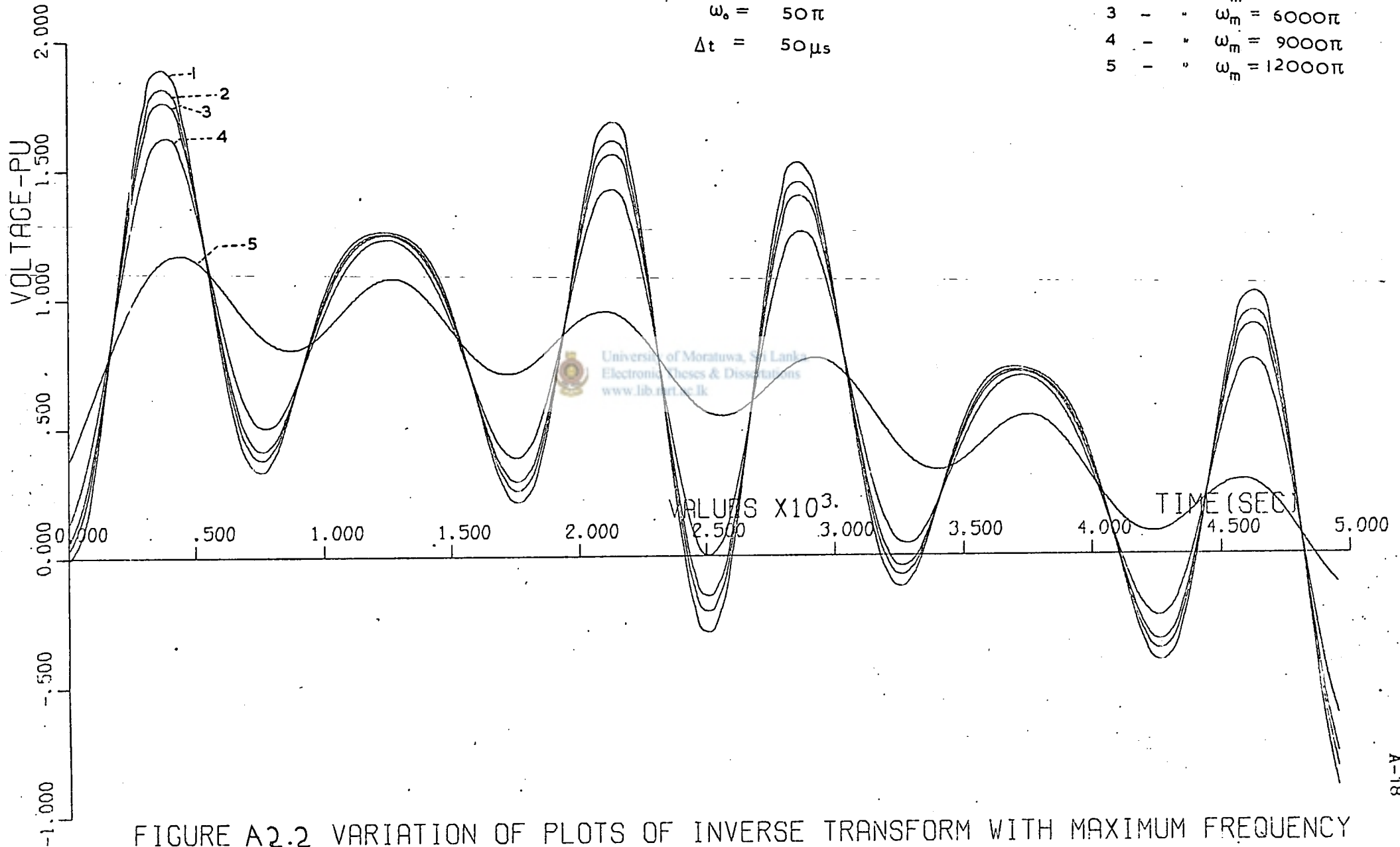
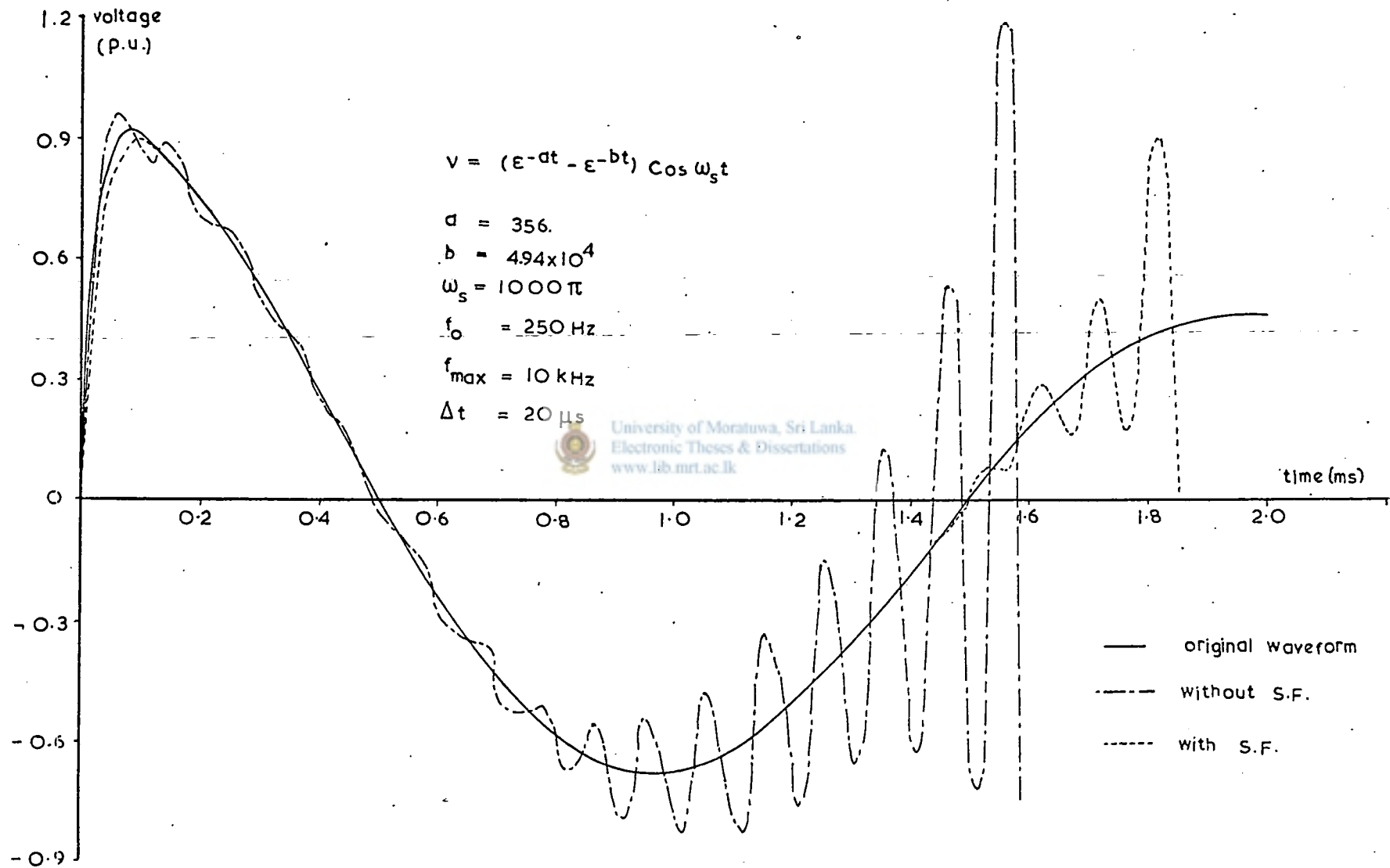


FIGURE A2.2 VARIATION OF PLOTS OF INVERSE TRANSFORM WITH MAXIMUM FREQUENCY



FigureA2.3 Effect of the Sigma Factor in Fourier Analysis

has a transform  $1/j\omega$ . When an upper limit  $\Omega$  is placed on the frequency spectrum, the inverse transform  $f_{\Omega}(t)$  is given by

$$f_{\Omega}(t) = \frac{2}{\pi} \operatorname{Re} \int_0^{\Omega} \frac{1}{j\omega} \cdot e^{j\omega t} d\omega$$

where  $\omega$  is the angular frequency

$$\text{i.e. } f_{\Omega}(t) = \frac{2}{\pi} \int_0^{\Omega} \frac{1}{\omega} \sin \omega t \cdot d\omega$$

If a change of variable  $x = \omega t$  is made in the above equation, it takes the form

$$f_{\Omega}(t) = \frac{2}{\pi} \int_0^{\Omega t} \frac{\sin x}{x} \cdot dx$$

which function contains the sine integral  $\operatorname{Si}(x)$ . Thus

$$f_{\Omega}(t) = \frac{2}{\pi} \cdot \operatorname{Si}(\Omega t)$$

Figure A2.4 shows a plot of  $\frac{2}{\pi} \operatorname{Si}(\Omega t)$  against  $\Omega t$ . This plot gives the variation of the inversion integral with time  $t$  for a given maximum frequency  $\Omega$ . On the otherhand, it also shows the effect of increasing the maximum frequency  $\Omega$  for a given time  $t$ . It is seen that the error increases substantially at very low values of the product  $\Omega t$ .

Figure A2.4 also shows how the standard sigma factor  $\sigma_{\text{std}}$  given by

$$\sigma_{\text{std}} = \frac{\sin(\omega/\Omega)\pi}{(\omega/\Omega)\pi}$$

improves the long term response at the expense of the initial rate of rise. When the standard sigma factor is used, the response  $f_{\sigma}(t)$  is the local average of  $f_{\Omega}(t)$  over each period of the maximum frequency  $\Omega$ . Since the maximum error occurs at minimum time, if the time step  $\Delta t$  is chosen corresponding to  $\Omega \cdot \Delta t \approx 4$ , not much error would occur in the response. However, when the response is taken over a large period (global response), a slight error in the initial rise time may not be of much significance and a lower value of  $\Omega \cdot \Delta t$  may be chosen to reduce computation.

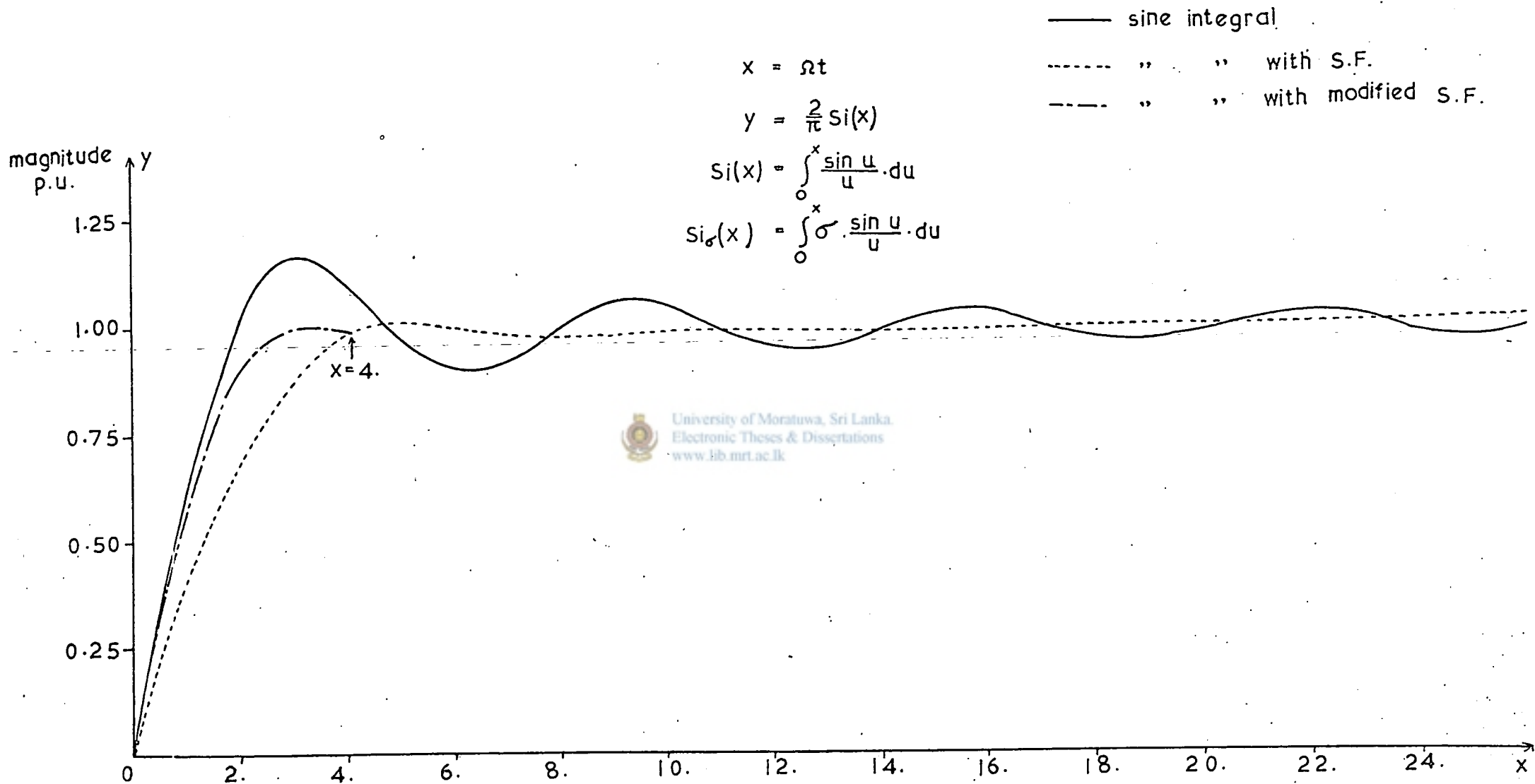


Figure A2.4 Plot of the sine integral

As is seen from figure A2.4, the sigma factor causes a much lower rate of rise below  $\Omega t$  equal to 4. Thus, a modified sigma factor  $\sigma_{\text{mod}}$  given by

$$\sigma_{\text{mod}} = \frac{\text{Sin } a w}{a w}$$

where  $a = t \frac{\pi}{4}$  for  $0 \leq \Omega t \leq 4$   
and  $a = \pi/\Omega$  for  $\Omega t \geq 4$

may be used to improve the initial rate of rise (figure A2.4), while keeping the long term response the same as for the standard sigma factor.

The inversion integrals with the standard and modified sigma factors, may also be expressed in terms of the Sine integral as

$$f_{\sigma}(t) = \frac{2}{\pi} \text{Si}_{\sigma}(\Omega t) = \int_0^{\Omega} \sigma \cdot \frac{\text{Sin } w t}{w} \cdot dw$$

for the standard sigma factor, which factor can also be shown equal to

$$f_{\sigma}(t) = \frac{2}{\pi} \left[ \left( \frac{1}{2} + \frac{\Omega t}{2\pi} \right) \text{Si}(\Omega t + \pi) + \left( \frac{1}{2} - \frac{\Omega t}{2\pi} \right) \text{Si}(\Omega t - \pi) \right]$$

and for the modified sigma factor can be shown to be equal to

$$f_{\sigma_{\text{mod}}}(t) = \frac{2}{\pi} \left[ -2 \text{Sin } \Omega t \cdot \frac{\text{Sin}(\frac{1}{2}\pi \Omega t)}{(\frac{1}{2}\pi \Omega t)} + \left( \frac{3}{2} + \frac{2}{\pi} \right) \text{Si}\left(1 + \frac{\pi}{4}\right) \Omega t + \left( \frac{3}{2} - \frac{2}{\pi} \right) \text{Si}\left(1 - \frac{\pi}{4}\right) \Omega t \right]$$

for  $0 \leq \Omega t \leq 4$

and  $f_{\sigma_{\text{mod}}}(t) = f_{\sigma}(t)$  for  $\Omega t \geq 4$

However, the modified sigma factor has been calculated on the basis of the frequency spectrum of the step wave. These do not necessarily apply for the switching surges, especially as there would be more than one discontinuity when sequential switching occurs. Since the modified sigma factor improves the rise time at the initial discontinuity only, and since since multiplicity of switching is involved in the present problem, the standard sigma factor has been used in the computation.

### A2.3 Shift Factor<sup>35</sup>

In the numerical form of the inversion integral, problems arise due to the fact that generally poles of the integrand lie close to the path of integration. This causes the integrand to peak at intervals along the path of integration and necessitates using a very small step length in the numerical integration. In the modified Fourier integral, the shift factor is used to move the path of integration away from the poles and hence smooth the integral and so enable the use of a greater step length (viz. in the time domain this corresponds to an exponential decay of the waveform so that a finite period may be considered). Figure A2.5 shows the effect of the shift factor on the frequency spectrum of the cosine waveform. It shows that the shift factor  $\alpha = 2\omega_0$  sufficiently smoothens the integral ( $\omega_0$  is the fundamental frequency of analysis). Figure A2.6 shows the decaying (1- Cosine) waveform for different exponential decay functions. When the decay is sufficiently large, the integral no longer peaks and the shift factor is no longer necessary. In theory, the value of the shift factor does not affect the result, but in practice due to the limits placed on the numerical integration, an optimum value of the shift factor may be chosen. While the shift factor is chosen sufficiently large to make the integration smooth and reduce integration errors, it must not be too large, as then the applied time decay would be faster than the decay of the truncation error term<sup>35</sup>, and when multiplied by  $\exp(\alpha t)$  as is required for the process, would result in an amplified truncation error.

### A2.4 Choice of Parameters

Consider the Fourier inversion integral, given by

$$f(t) = \frac{2}{\pi} \int_0^{\Omega} F(\omega) \cdot e^{j\omega t} d\omega$$



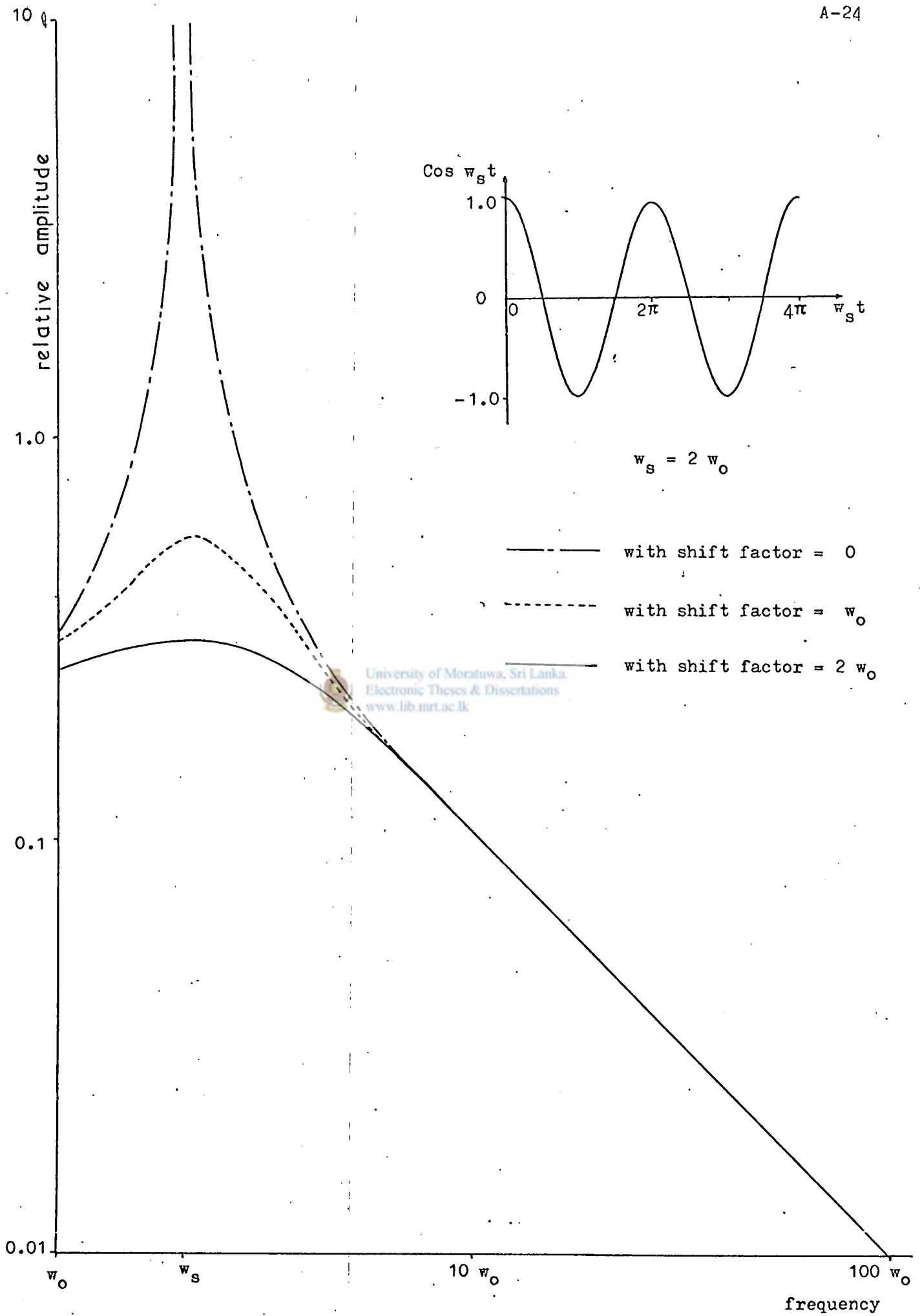


Figure A2.5 Frequency spectrum of cosine waveform (log scale)

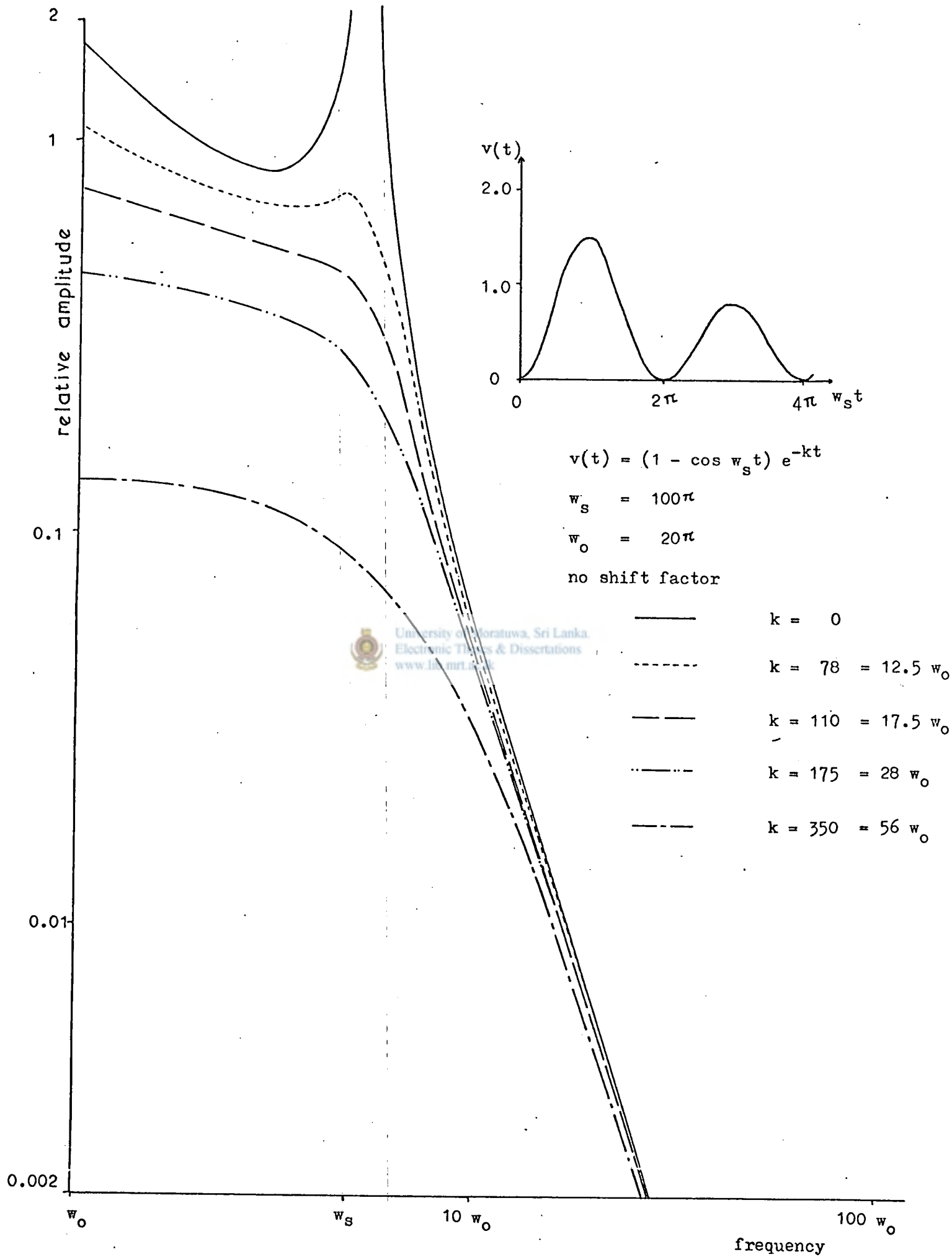


Figure A2.6 Frequency spectrum of decaying (1 - Cosine) waveform

If the substitution  $a(\omega, t) = \frac{2}{\pi} F(\omega) \cdot e^{j\omega t}$  is made, this becomes

$$f(t) = \int_0^{\Omega} a(\omega, t) d\omega$$

When integration is carried out numerically, a finite step length has to be chosen (say  $\Delta\omega = 2\omega_0$ ). The function may then be written in the form

$$f(t) = \sum_{i=1}^N a_{2i} \cdot 2\omega_0, \quad \text{where } a_i = a(i\omega_0, t)$$

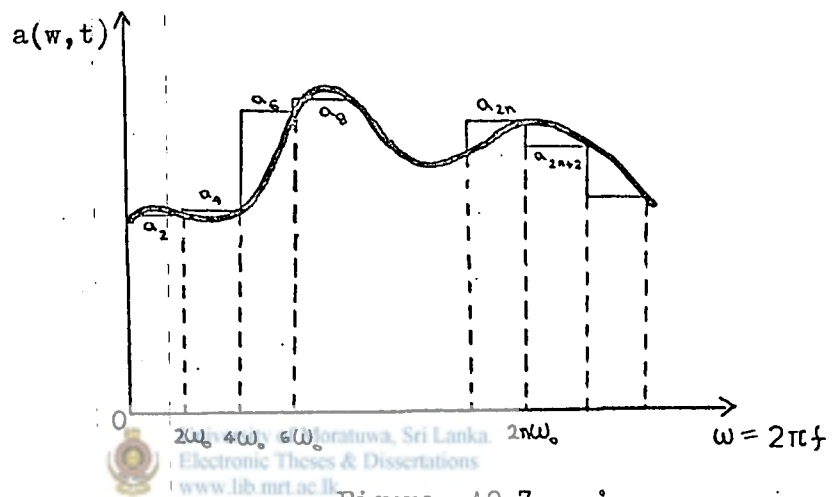


Figure A2.7

Figure A2.7 shows a numerical integration where the value of the function is assumed to remain constant for the whole of the previous interval at its value. However, a more satisfactory solution would be to assume the value constant at its value for half the previous period and half the following period. This is shown in figure A2.8.

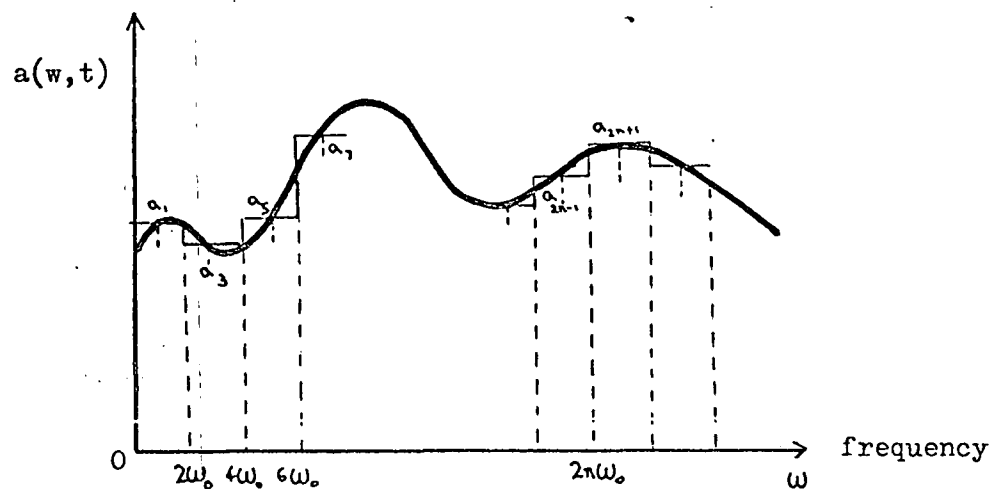


Figure A2.8

This evidently gives a better integration than the former. This latter form can be interpreted to mean that the frequency spectrum is calculated for odd harmonics of the basic frequency  $f_0$ . Since the step length has been limited to  $2f_0$ , repetition would occur (as in the Fourier series) after this period, and the maximum value of the observation time that could be considered is governed by this frequency. However, due to the discontinuity at the end of this time, Gibb's oscillation would occur (c.f. figure A.2.1). Thus the effective time of observation  $T_0$  is related to the frequency step length as

$$T_0 \leq \frac{1}{2f_0}$$

In practical problems, the Gibb's oscillation at the end of the waveform does not penetrate beyond half the period of observation, so that a choice  $T_0 \geq \frac{1}{4f_0}$  would be sufficient. Thus the basic frequency  $f_0$  may be chosen so as to satisfy

$$\frac{1}{2T_0} \geq f_0 \geq \frac{1}{4T_0}$$

Also, from the analysis of section A2.2 and from figure A2.3 it is apparent that a choice of  $\Omega \cdot \Delta t$  of about 4 would give adequate definition of waveform. If the maximum frequency that has to be considered is limited by system considerations, or if the types of waveforms likely to be obtained are known and their frequency spectrums are also known (such as with exponentials shown in figure A2.9), then the value of the time step required may be correspondingly chosen. This choice could be verified by a 'trial and error' method of halving the step length for time, and observing whether there is any significant change in the response.

A value of  $\alpha = 2 \omega_0$  has been chosen for the shift factor, as it has been seen to be satisfactory.

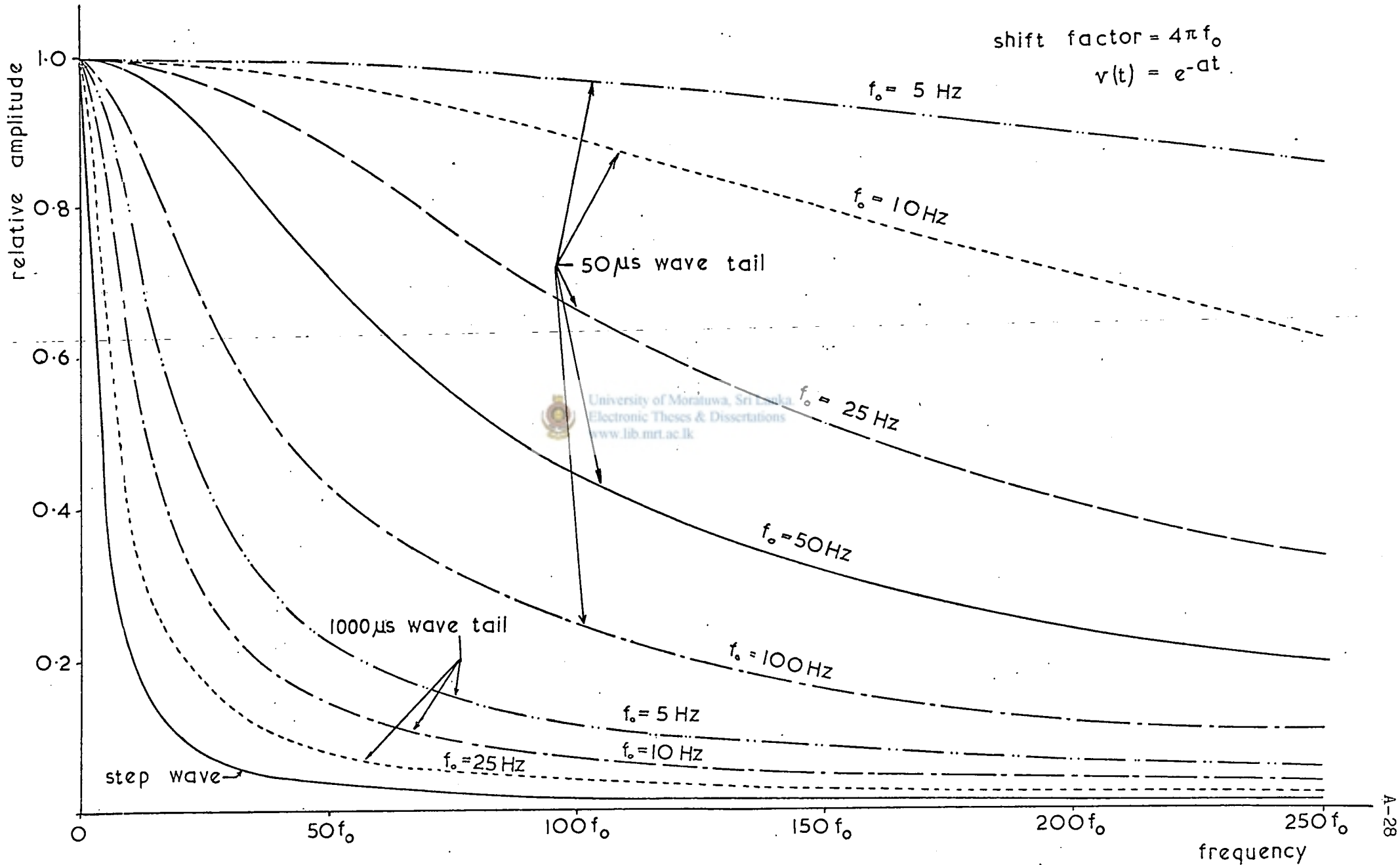


Figure A2.9 Frequency spectrum of exponential waveform (linear scales)

### A2.5 A Particular Problem

A particular problem may arise in the method of analysis used when a relatively long line is fed through a transformer, which causes the resonant frequency of the system to approach the supply frequency. In this case, it has been found during the present work that the inversion integral would peak heavily at the resonant frequency. It was attempted to resolve this problem by using a suitable shift factor to smooth the integrand.

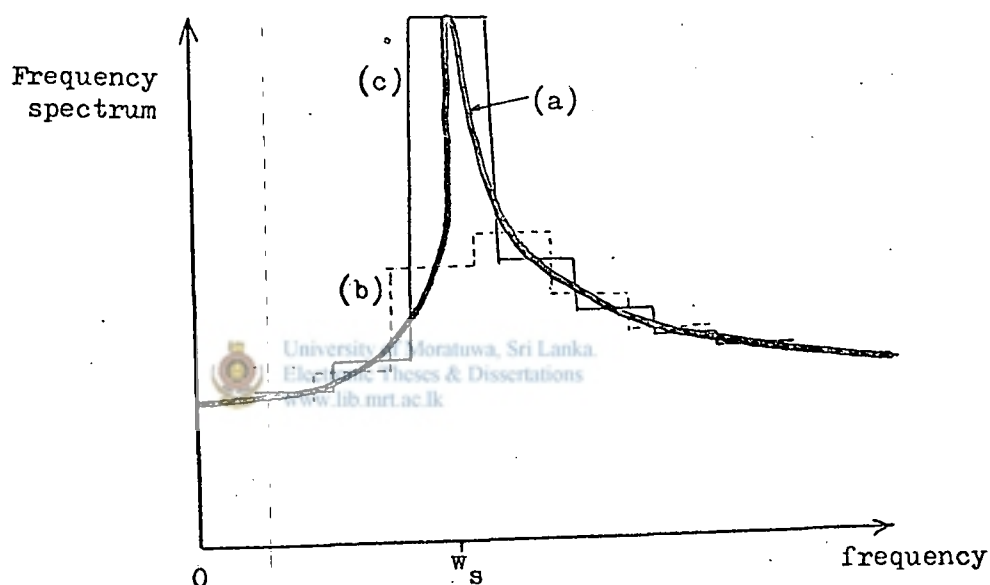


Figure A2.10

However, this was found to be unsatisfactory as a very large shift factor would be required to smooth the waveform. Since truncation errors are present, post-multiplying by the exponential function, as is required in the inversion integral, would result in amplified errors. Figure A2.10 (a) shows the typical form of the frequency spectrum mentioned above. In the integration, if too large a step length is chosen, either the peak may be completely bypassed (figure A2.10 (b)), or the integral may take a much higher value (figure A2.10 (c)). This problem may be avoided by choosing a sufficiently small step length. However, this would result

in a very large number of terms to be taken, if the high frequency components are not to be truncated completely. Computationally this would be extremely uneconomic. Under these circumstances, once the frequency at which peaking occurs is known, the following method may be used. The integral of the inverse transform is performed with variable frequency step length (figure A2.11).

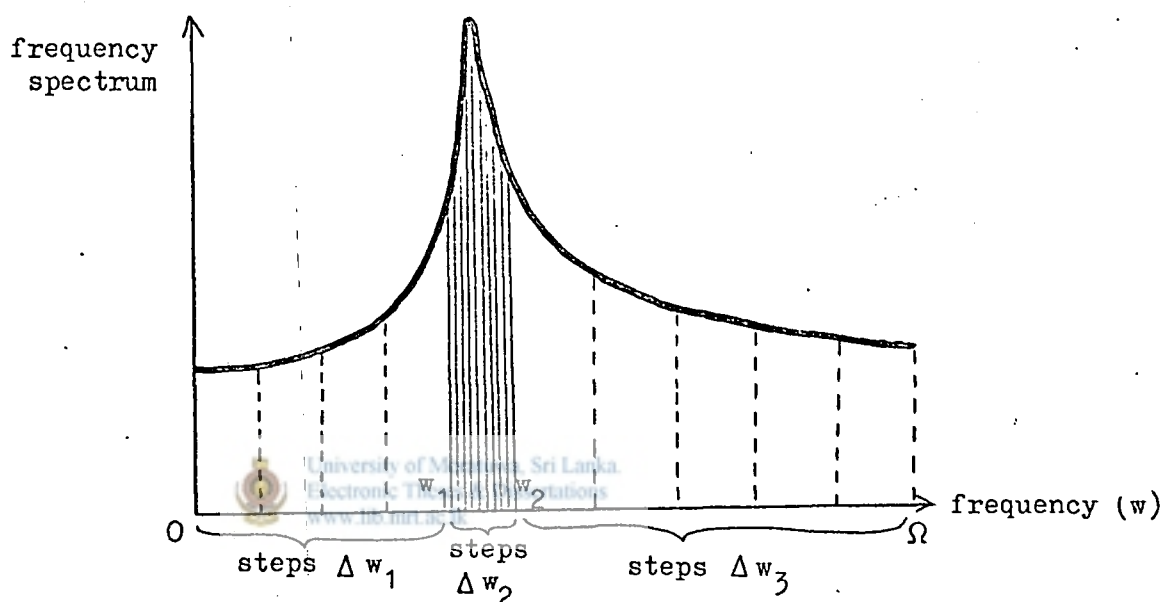


Figure A2.11

with variable step lengths  $\Delta w_1$ ,  $\Delta w_2$ , and  $\Delta w_3$  chosen, the inverse transform may be written as

$$\begin{aligned} f(t) &= \frac{2}{\pi} \int_0^{\Omega} F(w) \cdot e^{j\omega t} \cdot dw \\ &= \frac{2}{\pi} \left[ \sum_0^{w_1} F(w) \cdot e^{j\omega t} \cdot \Delta w_1 + \sum_{w_1}^{w_2} F(w) \cdot e^{j\omega t} \cdot \Delta w_2 + \sum_{w_2}^{\Omega} F(w) \cdot e^{j\omega t} \cdot \Delta w_3 \right] \end{aligned}$$

A very small step length is chosen for the region  $w_1$  to  $w_2$ , while for the rest, a moderate step length may be chosen.

APPENDIX 3LEAKAGE INDUCTANCE AND MUTUAL COUPLINGA3.1 Introduction

Although the term 'leakage inductance' has been used widely in transformer literature, as Ganz<sup>70</sup> indicates, there is still a disagreement to its meaning. As such for the purposes of the present work, the term 'leakage inductance' is defined as indicated below.

For a single phase of the transformer, it is possible to derive both an exact T-equivalent circuit and an exact  $\pi$ -equivalent circuit taking into consideration the inductive coupling.

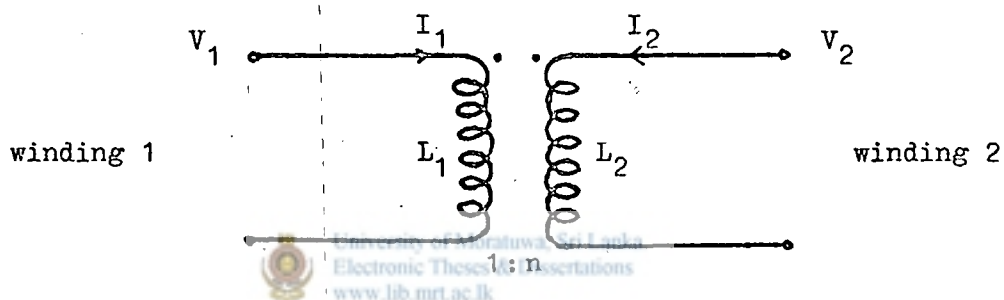


Figure A3.1

For the transformer shown in figure A3.1, let

- $L_1, L_2$  - self inductance of windings 1 and 2 respectively
- $M$  - mutual inductance between windings 1 and 2
- $n$  - turns ratio of windings (nominal voltage ratio)
- $I_1, I_2$  - currents in the windings 1 and 2 respectively
- $V_1, V_2$  - voltages across the windings 1 and 2 respectively.

Then it is possible to relate the voltages and the currents by the differential equations

$$L_1 p I_1 + M p I_2 = V_1$$

$$M p I_1 + L_2 p I_2 = V_2$$

where  $p$  is the differential operator  $d/dt$ .



In the transformer, the primary winding and the secondary winding may or may not be wound on the same leg. Also where they are wound on the same leg, they may be wound in spiral, cross-over, helical or continuous disc form. Depending on the configuration of the windings, the relation between the self-inductance of the windings, the mutual inductance between the windings and the leakage inductance differ. However, under all these conditions the self inductance of the windings for most practical purposes, may be assumed to be related to each other in the proportion of the square of the turns. However, the mutual coupling has to take into account the effective leakage between the phase windings, which is dependant on the type of construction, by the use of a coupling factor, which factor is very near unity for modern power transformers.

### A3.2 Exact T-equivalent circuit

If  $k$  is the coefficient of coupling of the primary flux with the secondary, all inductances may be defined in terms of the primary self inductance  $L_1$  as

$$L_2 = n^2 L_1$$

$$M = k n L_1$$

Hence, the differential equations may be rewritten as

$$L_1 p I_1 + k n L_1 p I_2 = V_1$$

giving, with selected grouping of terms

$$V_1 = (1-k) L_1 p I_1 + k L_1 p (I_1 + n I_2) \quad (A3.1)$$

$$\text{similarly } V_2 = (1-k) L_2 p I_2 + k L_2 p (I_2 + I_1/n) \quad (A3.2)$$

which may be represented by the exact T-equivalent circuit in figure A3.2 .

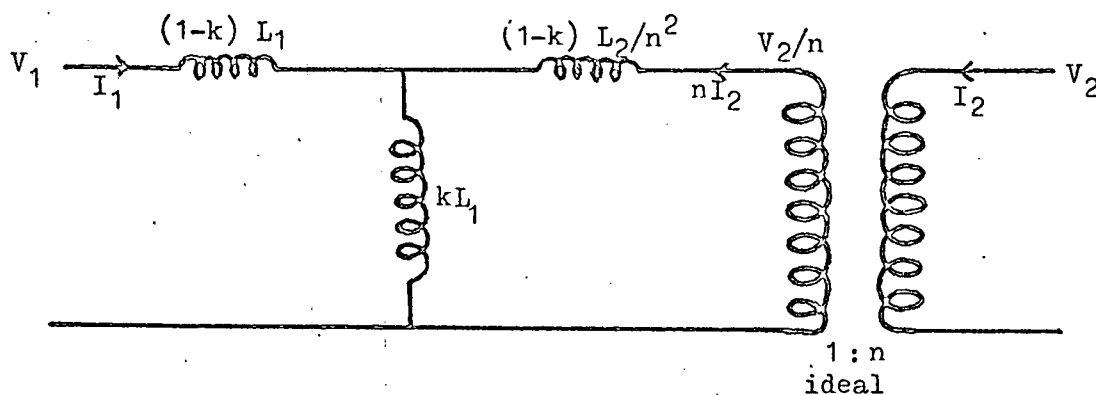


Figure A3.2

The series elements of the equivalent circuit of figure A3.2 may be defined as the leakage inductance of the primary and secondary sides, and the shunt element may be taken to represent the mutual coupling.

### A 3.3 Exact $\pi$ - equivalent circuit

It is also possible to write the differential equations as

$$\begin{bmatrix} I_1 \\ I_2 \end{bmatrix} = \begin{bmatrix} L_1 & M \\ M & L_2 \end{bmatrix}^{-1} \begin{bmatrix} V_1 \\ V_2 \end{bmatrix} = \frac{1}{L_1 L_2 - M^2} \begin{bmatrix} n^2 & -kn \\ -kn & 1 \end{bmatrix} \frac{1}{n^2(1-k^2)} \begin{bmatrix} V_1 \\ V_2 \end{bmatrix}$$

from which matrix equation

$$I_1 = \frac{1}{(1-k^2)L_{2p}} \left[ n^2(1-k)V_1 + kn^2(V_1 - V_2/n) \right]$$

$$\text{and } nI_2 = \frac{1}{(1-k^2)L_{2p}} \left[ -kn^2(V_1 - V_2/n) + n^2(1-k)V_2/n \right]$$

These equations may again be written as

$$I_1 = \frac{V_1}{(1+k)L_{1p}} + \frac{k}{(1-k^2)L_{1p}} (V_1 - V_2/n)$$

$$\text{and } -nI_2 = \frac{k}{(1-k^2)L_{1p}} (V_1 - V_2/n) - \frac{V_2}{n(1+k)L_{2p}}$$

which may be expressed by the exact  $\pi$  - equivalent circuit shown in figure A3.3 .

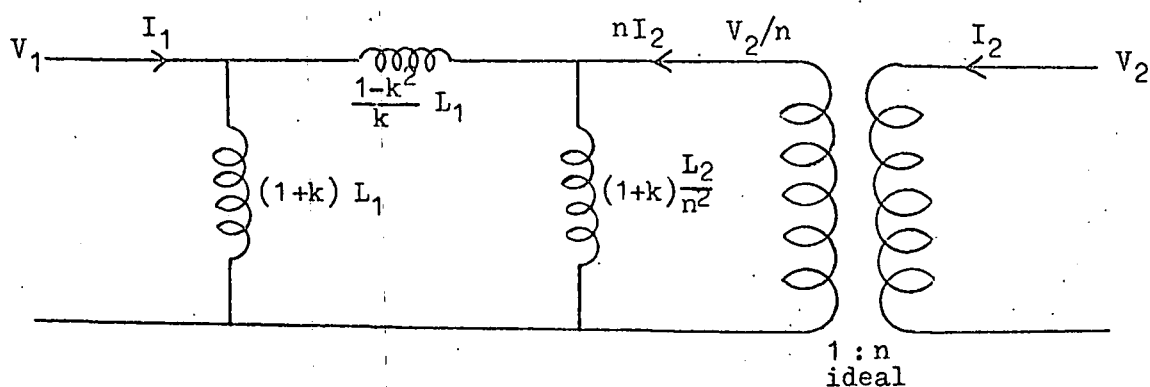


Figure A3.3

Here again, the series element may be defined as the leakage inductance, and the shunt branches as the magnetising inductance of the windings.

#### A 3.4 Comparison of Representation

When close coupling is achieved,  $k \approx 1$ , so that the total leakage inductance according to the T-circuit is

$$(1-k) L_1 + (1-k) L_2/n^2 = 2(1-k) L_1$$

and according to the  $\pi$ -circuit is

$$\frac{1-k^2}{k} L_1 = (1-k) \frac{(1+k)}{k} \approx 2(1-k) L_1$$

also for the shunt branches, the two methods give the mutual inductance referred to the primary as

$$\frac{(1+k)}{2} \cdot L_1 \approx kL_1 \approx L_1$$

Thus for close coupling, both circuits could have their series elements defined as 'leakage inductance'. However, when the coefficient of coupling decreases, figure A3.4 shows that they depart from each other. The figure also compares the 'leakage inductance' as obtained from the series branches of these two circuits with the 'short-circuit leakage inductance' defined by short-circuiting the secondary winding. In this case the reactance of the circuit is defined as the leakage reactance, and from equations A3.1 and A3.2 it is obtained as being equal to  $(1-k^2)L_1$ .

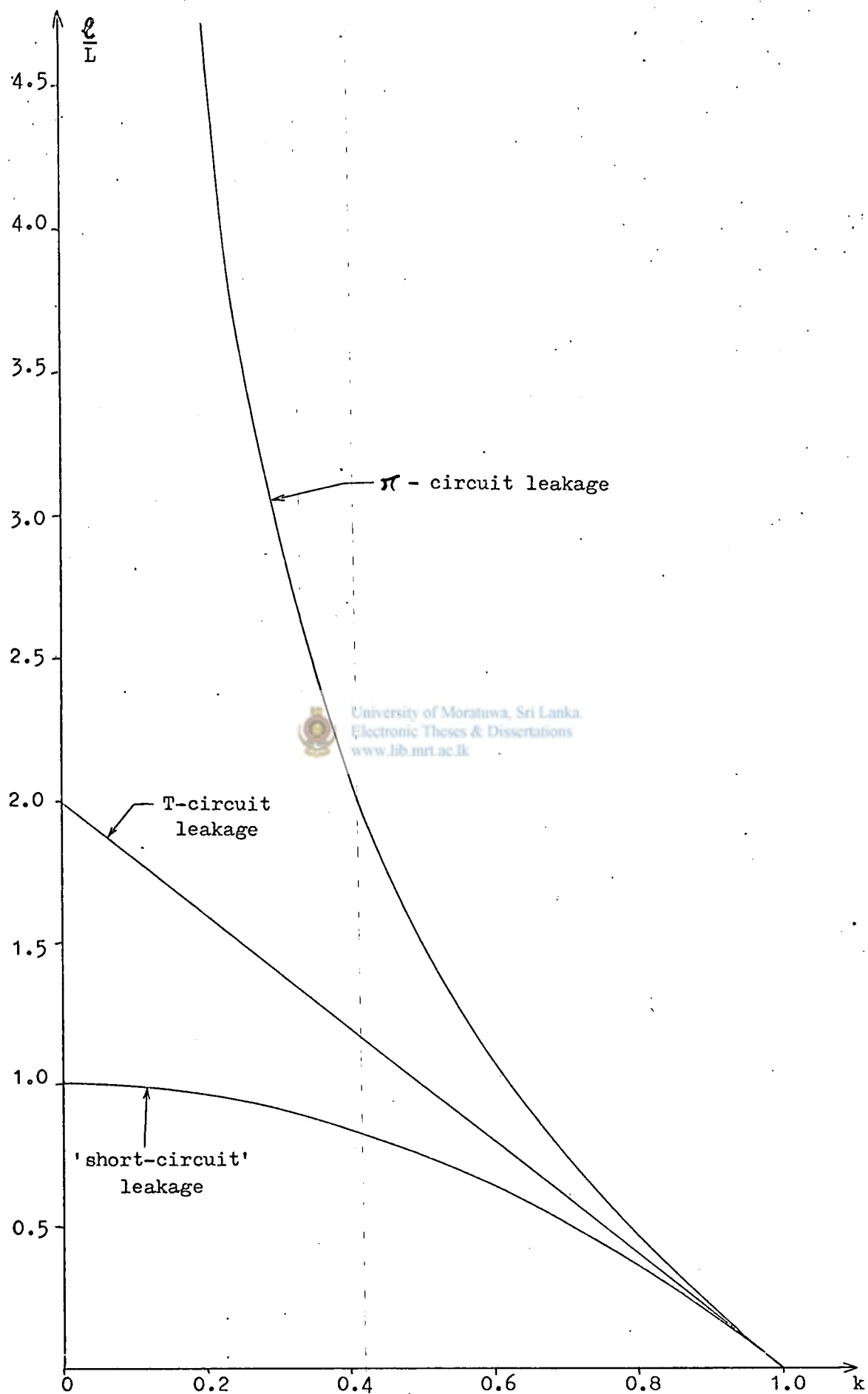


Figure A3.4 Plot of leakage inductance against coupling coefficient

If the coupling is very tight ( $k = 1$ ) between the two windings, there will be no leakage flux, which is verified by all three methods of definition. However, when coupling is very weak ( $k \approx 0$ ) there is no mutual flux so that the whole of the inductance would be leakage, the leakage being defined as that due to the flux linking one winding but not the other. The definition  $(1-k^2) L_1$  corresponding to the short-circuit case agrees with this deduction and the T-circuit definition would give twice the result. In this instance the  $\pi$ -circuit definition of leakage inductance would give a completely false result. Since for a transformer the coupling is almost unity on the same leg and quite close when separate limbs are involved, the definition of leakage inductance from the T-circuit may be accepted. However, the present work considers the 'short-circuit leakage inductance' to be the most appropriate.

University of Moratuwa, Sri Lanka  
Electronic Theses & Dissertations  
www.lib.mrt.ac.lk

### A3.5 Frequency dependance of inductance

Experiments<sup>47-49</sup> have shown that both self-inductance and mutual inductance vary with frequency, while the leakage inductance remains virtually constant. It can be shown, using a semi-logarithmic plot, that the variation of inductance with frequency follows an exponential law of the form

$$M = M_0 e^{-af}$$

- where
- $M_0$  - d.c. value of mutual inductance
  - $M$  - mutual inductance at frequency  $f$
  - $f$  - frequency in Hertz
  - $a$  - constant parameter dependant on material of core.

For practical purposes, the value of inductance at supply may be taken as  $M_0$ .

Both the mutual inductance and the self-inductance follow the same form of frequency dependence (figure A3.5). However, if the mutual inductance and the self inductance are allowed to vary independently, this would result in a frequency dependant leakage inductance. As such the variation of the self inductance is obtained from the variation of the mutual inductance and the constant leakage inductance.

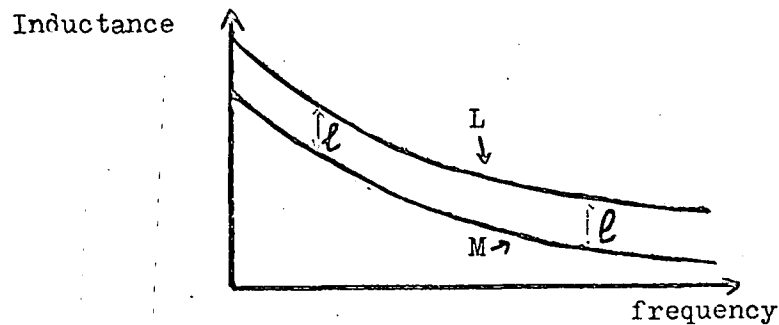


figure A3.5

Since, for switching surges which are considered in the present study, the frequencies of interest do not extend to very high frequencies, the coupling of flux between windings remains comparatively high, and the variation of the self-inductance may be obtained as

$$L = M + e$$

where all inductance values are referred to the same winding.

In general, due to the symmetrical form of the inductance matrix for the transformer, it is possible to account for the frequency dependant self-inductance and mutual inductance elements directly in the inverse inductance matrix, thus making the computation process simpler.

Although only a particular form of variation of self-inductance has been mentioned, due to lack of sufficient data on this variation, any other form of variation, if known, may be substituted without any difficulty into the computer program.

### A 3.6 Interphase Mutual Coupling

So far only the mutual coupling between windings on the same phase has been considered. When the mutual inductive coupling between windings on adjacent phases (separate limbs) are considered, separate considerations are necessary. The mutual coupling is no longer related to the self inductance through the leakage inductance but is calculated on the reluctance of the magnetic and air paths.

Consider for example a three-limb core (figure A3.6a), with windings on limbs 1 and 2 (considered having equal turns for simplicity of presentation). The limbs are sectioned as illustrated in figure A3.6b for the purpose of calculating the reluctances.

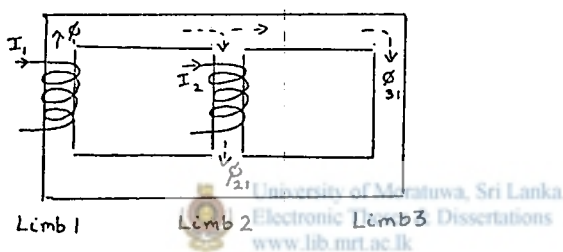


Figure A3.6a

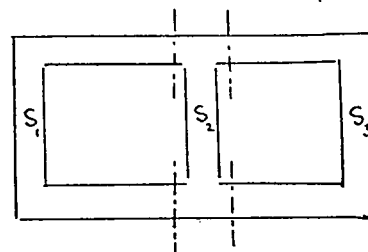


Figure A3.6b

Let

- $\phi_1$  - Flux linkage produced by current in winding 1
- $\phi_{21}$  - Flux linkage with limb 2 due to current in winding 1
- $\phi_{31}$  - Flux linkage with limb 3 due to current in winding 1
- $S_1, S_2, S_3$  - Reluctances of the 3 limbs (sectioned as illustrated)
- $I_1, I_2$  - Currents in windings 1 and 2 respectively
- $k_1$  - Interphase inductive coupling factor of flux from limb 1 to other cores (order of 0.8 to 1.0)

Equating flux linkage, when winding on limb 1 is energised, we have

$$\phi_{21} + \phi_{31} = k_1 \phi_1$$

Also, assuming the flux distribution in the other cores as inversely

proportional to the reluctances, we have

$$\frac{\phi_{21}}{\phi_{31}} = \frac{S_3}{S_2}$$

substitution and grouping terms gives

$$\phi_{21} \left( 1 + \frac{S_2}{S_3} \right) = k_1 \phi_1$$

$$\therefore \phi_{21} = \frac{k_1 \phi_1}{1 + S_2/S_3}$$

Thus the mutual inductance is given by

$$M_{21} = \frac{\phi_{21}}{I_1} = k_1 \cdot \frac{1}{1 + S_2/S_3} \cdot \frac{\phi_1}{I_1} = k_1 \cdot \frac{1}{1 + S_2/S_3} \cdot L_1$$

which expression takes into account the assymetry of the core, due to the difference in the reluctance paths of the inner and outer legs.

Similarly, if the winding on limb 2 is energised, it may be shown that

$$M_{12} = k_2 \cdot \frac{1}{1 + S_1/S_3} \cdot L_2$$

It is thus seen that the mutual coupling between the windings is not symmetric. It is also worth noting that the self inductances of the centre limb and of the outer limbs are different due to the assymetry of the core.





APPENDIX 4TRANSMISSION LINE PARAMETERS

The following sections describe the calculation of the Series impedance matrix  $Z$  and the Shunt admittance matrix  $Y$ , per unit length of an overhead transmission line.

A4.1 Series Impedance Matrix Per Unit Length

The calculation of the series impedance matrix for the transmission line is quite complex<sup>36</sup> due to the frequency dependence of the conducting paths. The various components of this matrix, calculated as described by Galloway et al<sup>71</sup>, are detailed below.

$$Z = Z_c + Z_g + Z_e$$

(i) The self impedance of the conductors,  $Z_c$ , is a diagonal matrix and is evaluated differently for low frequency (below 500 Hz) and high frequency ranges, due to the variation of current in the Conductor.

For low range of frequencies, the conductor self impedance is given to a good approximation by

$$Z_c = R_{dc} + \frac{j\omega\mu_0}{2\pi} \log_e(r/r_{gm})$$

where

$r$  = overall conductor radius

$r_{gm}$  = mean geometric radius corresponding to stranding

$R_{dc}$  = resistance per unit length, to direct current =  $\rho_c/n\pi r_s^2$

$\rho_c$  = resistivity of conductor metal

$r_s$  = radius of individual strand

$n$  = total number of conducting strands (steel strands neglected).

For the higher range of frequencies, due to skin effect, the current is confined to the surface of outer layers of the conductor, and the corresponding formula for the self impedance is quite accurately given by

$$Z_c = K \rho m / r_s \pi (n_o + 2)$$

where

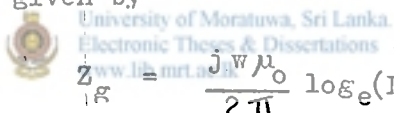
$K$  = stranding factor to account for non-uniform field distribution on the circumference ( $K \approx 2.25$  experimentally)

$$m = (j \omega \mu_o \mu_r / \rho)^{\frac{1}{2}}$$

$n_o$  = number of strands in outer layer

$\mu_r$  = relative permeability of conductor material.

(ii) The impedance due to the electromagnetic coupling between conductors,  $Z_g$ , is given by



$$Z_g = \frac{j \omega \mu_o}{2 \pi} \log_e (D/d)$$

where

$D_{ij}$  = distance between conductor  $i$  and the image of conductor  $j$ ,

$d_{ij}$  = distance between two conductors  $i$  and  $j$ ,  $i \neq j$ , or  
= radius of conductor, when  $i = j$ .

(iii) The impedance due to the electromagnetic coupling of the conductors with the earth,  $Z_e$ , is calculated according to Carson's formula<sup>50</sup> by the expression

$$Z_e = \frac{\omega \mu_o}{2 \pi} (P + j Q)$$

The infinite series defined overleaf are terminated after a sufficient convergence has been reached.

where

P and Q = matrices calculated from series which are functions of two parameters  $r_{ij}$  and  $\theta_{ij}$ ,

such that

$$r_{ij} = (\omega \mu_0 / \rho)^{\frac{1}{2}} D_{ij}$$

and  $\theta_{ij}$  = angle subtended at the  $i^{\text{th}}$  conductor by the images of the  $i^{\text{th}}$  and  $j^{\text{th}}$  conductors.

Note: For different ranges of frequency, the matrices P and Q are obtained by different series<sup>71</sup>.

#### A4.2 Shunt Admittance Matrix Per Unit Length

The shunt admittance due to the capacitive coupling between the conductors and their images in a perfect earth is a function of the physical geometry of the conductors relative to the earth plane<sup>71</sup>, and are given by

$$Y = j \omega 2\pi \epsilon / \log_e(n/d)$$

where

$Y_{ij}$  =  $(i,j)^{\text{th}}$  element of the shunt admittance matrix Y,

$\epsilon$  = permittivity of conductor

$D_{ij}$  = distance between the  $i^{\text{th}}$  conductor and the image of j,

$d_{ij}$  = distance between the  $i^{\text{th}}$  and  $j^{\text{th}}$  conductors,  $i \neq j$ , or  
= radius of conductor, for  $i = j$ .

#### A4.3 Bundle Conductors

When the bundle conductor is considered, as is usual for the high voltage lines, the corresponding radius for the calculation of the 'self' terms, in the matrices of the above sections, will be the equivalent radius of the bundle given by the geometric mean radius<sup>36</sup>. Also, the self-impedance calculation carried out for the single conductor, has its value divided by the number of conductors in the bundle to obtain the equivalent self impedance of the phase.



APPENDIX 5CABLE PARAMETERS

Unlike in the transmission line, the calculation of the parameters for the cable is more complicated due to the presence of the additional media such as the conductor dielectric, sheath and sheath dielectric.

A5.1 Series Impedance Matrix Per Unit Length

For the cable, the exact expressions for the series impedance involve the Bessel functions and functions of the Bessel functions<sup>72</sup>. However, simplified solutions are available which are applicable over a wide range of frequencies. The different components of the series impedance matrix are described below.

(i) The internal impedance,  $Z_c$ , of the conductor is quite accurately given by the expression<sup>31</sup>

$$Z_c = \frac{\rho_1 m}{2\pi r_1} \coth(0.777 m r_1) + \frac{0.356 \rho_1}{\pi r_1^2}$$

where

$\rho_1$  = resistivity of inner conductor,

$m = (j \omega \mu / \rho_1)^{\frac{1}{2}}$

$r_1$  = radius of inner conductor

In particular, for very high frequency ( $\omega \mu / \rho_1 \gg 1$ ), the above formula reduces to the familiar skin effect formula  $Z_c = \rho_1 m / 2\pi r_1$ , and at very low frequency (or for d.c.) at which  $\omega \mu / \rho_1 \ll 1$ , the above gives the expression for the d.c. resistance  $Z_c = \rho_1 / \pi r_1^2$ .

(ii) The magnetic flux in the conductor dielectric gives rise to the conductor-sheath mutual impedance,  $Z_{sc}$ , which is given by the expression

$$Z_{sc} = \frac{j \omega \mu}{2 \pi} \log_e(r_2/r_1)$$

where  $r_2$  = inner radius of sheath.

(iii) The inner, surface sheath impedance,  $Z_{si}$ , is approximately given by

$$Z_{si} = \frac{\rho_2 m}{2 \pi r_2} \text{Coth}(m(r_3 - r_2)) - \frac{\rho_2}{2 \pi r_2 (r_3 + r_2)}$$

where

$$m = (j \omega \mu / \rho_2)^{\frac{1}{2}}$$

$\rho_2$  = resistivity of sheath

$r_3$  = outer radius of sheath



University of Moratuwa, Sri Lanka  
Electronic Theses & Dissertations  
www.lib.mrt.ac.lk

(iv) Due to the current flow in the sheath, a voltage is induced in the sheath-earth path giving rise to the mutual impedance between inner and outer sheath surfaces. This impedance,  $Z_m$ , is given by the expression

$$Z_m = \frac{\rho_2 m}{(r_2 + r_3)} \text{Cosech}(m(r_3 - r_2))$$

(v) The outer, surface sheath impedance,  $Z_{so}$ , is given by the approximate expression

$$Z_{so} = \frac{\rho_2 m}{2 \pi r_3} \text{Coth}(m(r_3 - r_2)) + \frac{\rho_2}{2 \pi r_3 (r_3 + r_2)}$$

(vi) The flux in the sheath dielectric causes a mutual impedance between the sheath and earth,  $Z_{se}$ , and is given by the formula

$$Z_{se} = \frac{j \omega \mu}{2 \pi} \log_e (R/R_3)$$

where  $R$  = overall radius of cable, and radius of earth return path.

(vii) The earth return path has an impedance,  $Z_e$ , which may be represented by the following expression

$$Z_e = \frac{j \omega \mu_0}{2 \pi} (6.4905 - \log_e p + K q - j(\frac{1}{2} - K q))$$

where

$$q = (f/\rho_e)^{\frac{1}{2}}$$

$$f = \text{frequency (Hz)}$$

$$p = q \cdot d$$

$$d = \text{distance between cables}$$

$$K = 0.0013245(b + c)$$

$$b = \text{depth of inducing cable (b is negative)}$$

$$c = \text{depth of induced cable (c is negative)}$$

If the earth is taken as reference, the series impedance per unit length of each cable is given by the matrix (with rows and columns indicated by  $c$  and  $s$  referring to the core and sheath quantities respectively)

$$Z = \begin{matrix} & \begin{matrix} c & s \end{matrix} \\ \begin{matrix} c \\ s \end{matrix} & \begin{bmatrix} Z_{11} & Z_{12} \\ Z_{12} & Z_{22} \end{bmatrix} \end{matrix}$$

where

$$Z_{11} = Z_c + Z_{sc} + Z_{si} + Z_{so} + Z_{se} + Z_e - 2 Z_m$$

$$Z_{12} = Z_{so} + Z_{se} + Z_e - Z_m$$

$$Z_{22} = Z_{s0} + Z_{se} + Z_e$$

Due to the magnetic flux, there is a substantial mutual impedance between adjacent cables, which is highly dependent on frequency. These may be calculated in a way similar to that described in the foregoing sections. By combining the impedance matrices for the individual cables with the mutual impedance matrices, the complete impedance matrix per unit length may be obtained.

#### A5.2 Shunt Admittance Matrix Per Unit Length

Evaluation of the shunt admittance matrix is quite straight forward. The three conducting paths (core, sheath and earth) form equipotential surfaces. If the dielectric loss is neglected, then the conductor-sheath shunt admittance,  $Y_{cs}$ , and the sheath-earth shunt admittance,  $Y_{se}$ , are readily given by the expressions<sup>31</sup>

$$Y_{cs} = \frac{j \omega 2 \pi \epsilon_1}{\log_e (r_2/r_1)}$$

$$Y_{se} = \frac{j \omega 2 \pi \epsilon_2}{\log_e (R/r_3)}$$

where

$\epsilon_1$  = permittivity of conductor dielectric,

$\epsilon_2$  = permittivity of sheath dielectric.

If the earth is taken as reference, the shunt admittance matrix per unit length of each cable is given by

$$Y = \begin{matrix} & \begin{matrix} c & s \end{matrix} \\ \begin{matrix} c \\ s \end{matrix} & \left[ \begin{array}{cc} Y_{cs} & -Y_{cs} \\ -Y_{cs} & Y_{cs} + Y_{se} \end{array} \right] \end{matrix}$$



As the earth return path may be considered as an electrostatic screen, there is no mutual admittance between adjacent cables. Thus for the three phase cable, the block matrix derived above is compounded to form a diagonal matrix.

### A5.3 Earth-Continuity Cable

The earth continuity conductor, if present, consists of an inner conductor, conductor dielectric and sheath. The impedance of this conductor consists of the internal conductor impedance, the impedance due to the magnetic flux, and that due to the earth return path.

The series impedance and the shunt admittance components have forms similar to those described in the foregoing sections and are calculated as such.

APPENDIX 6ELIMINATION OF EARTH CONDUCTORS AND SHEATHS IN  
TRANSMISSION LINES AND CABLES FROM MATRIX

In general, the series impedance and shunt admittance matrices calculated for transmission lines and cables (Appendices 4 & 5 ) will include elements corresponding to earth conductors, sheaths etc., in addition to those corresponding to the phase conductors. In the case of earth conductors, as well as sheaths in cross-bonded cables, regular earthing is effected at points along their lengths. These conductors would thus have potentials near zero, especially at the transmission towers or points of earthing. It is possible to have standing voltage waveforms along their lengths, but since switching surges are of interest, these are thought to be extremely small. An accurate method of reduction of the matrices so as to contain modified terms corresponding only to the phase conductors would be to divide the line or cable into sections corresponding to tower spans or bonding sections and substitute the terminal conditions at these points. In the case of cross-bonded cables, non-linear cable covering protection units would need to be represented at these points. However, this is considered to be computationally extravagant. Another possibility is to consider zero voltage or suitable earthing resistance only at the two ends of the line and apply these boundary conditions to the two port admittance matrix equations, derived including the additional elements for the earth conductors.

$$\begin{bmatrix} I_{\sim sp} \\ I_{\sim se} \\ I_{\sim rp} \\ I_{\sim re} \end{bmatrix} = \begin{bmatrix} [A] & -[B] \\ -[B] & [A] \end{bmatrix} \begin{bmatrix} V_{\sim sp} \\ V_{\sim se} \\ V_{\sim rp} \\ V_{\sim re} \end{bmatrix}$$

suffixes s, r refer to the sending and receiving ends respectively  
 suffixes p, e refer to the phase conductors and earth conductors

However this is not much more accurate than assuming zero voltage throughout the length of the conductor. Thus the reduction of the impedance and admittance matrices to eliminate these earth conductors is based on this latter assumption.

In the case of admittance matrices, this assumption is easily accommodated by removing the rows and columns corresponding to earth conductors and/or sheaths, giving a reduced equivalent admittance matrix. However, in the case of the impedance matrix, the elimination of the earth-wire and/or sheaths from the matrix equations without disturbing their shielding properties is done by first inverting the impedance matrix and then proceeding as an admittance matrix. Finally, the reduced matrix is re-inverted to provide the corrected impedance matrix which allows for the effects of sheaths and/or earth wires. In fact, it will be shown that this double inversion process can be dispensed with, and in its place the original matrix may be modified suitably to give the same desired result.

For example, consider an  $(m + n)$  conductor system, where  $n$  conductors have zero voltage along their length. The impedance matrix may be written as

$$Z = \begin{bmatrix} Z_A & Z_B \\ Z_C & Z_D \end{bmatrix}$$

where

$Z_A$  = self-impedance matrix of the non-zero voltage conductors  
order of matrix (m x m).

$Z_B, Z_C$  = matrices of mutual impedance between the zero-voltage  
and the non-zero voltage conductors. Order (mxn) & (nxm).

$Z_D$  = self impedance matrix of the zero-voltage conductors  
order of matrix (n x n).

We are infact interested in only the (m x m) submatrix of  
the inverse of the above impedance matrix, as this then inverted gives  
the desired result. Well known matrix theory could be used to show  
that the first (m x m) submatrix of the inverse is given by

$$(Z_A - Z_B \cdot Z_D^{-1} \cdot Z_C)^{-1}$$

and, thus the required reduced impedance matrix is given by

$$(Z_A - Z_B \cdot Z_D^{-1} \cdot Z_C)$$

This result suggests that instead of computing two inversion processes,  
a single inversion of a much smaller matrix  $Z_D$  and two matrix  
multiplications is all that is now required.

The result derived above has been used extensively in the  
computer programs of the present study, where zero voltages (and sometimes  
even zero currents, with corresponding admittance matrices) are involved.  
For this technique to be used, all the impedances corresponding to zero  
voltages (or admittances corresponding to zero currents) must be placed at  
the extreme rows and columns of the original matrix.

APPENDIX 7MULTICONDUCTOR WAVE EQUATIONS

The theory of modal analysis proposed by Wedepohl<sup>43</sup> provides a completely generalised method of solving the travelling wave phenomena on multiconductor lines. In this method, the problem is reduced to the simple case of independent differential equations by a linear transformation.

The voltages and currents at any point  $x$  along a homogeneous multiconductor transmission line are inter-related by

$$\frac{dV}{dx} = -Z I \quad (A7.1)$$

$$\frac{dI}{dx} = -Y V \quad (A7.2)$$

where

- $V, I$  = column vectors of  $n$  elements of voltage and current  
 $Z, Y$  = system series impedance and shunt admittance matrices  
 $n$  = number of conductors in multiconductor system.

Differentiating the equations A7.1 and A7.2 with respect to  $x$  and subsequent eliminations yield the second order differential equations

$$\frac{d^2V}{dx^2} = Z Y \cdot V = P \cdot V \quad (A7.3)$$

$$\frac{d^2I}{dx^2} = Y Z \cdot I = P^t \cdot I \quad (A7.4)$$

where  $P = Z Y$ , and it can be shown that  $P^t = Y Z$ .

The differential equations A7.3 and A7.4 have solutions of the

form given below

$$V = \exp(-P^{\frac{1}{2}} x) \cdot V_i + \exp(P^{\frac{1}{2}} x) \cdot V_r \quad (A7.5)$$

$$I = Y_0 \left[ \exp(-P^{\frac{1}{2}} x) \cdot V_i - \exp(P^{\frac{1}{2}} x) \cdot V_r \right] \quad (A7.6)$$

where

$$Y_0 = Z^{-1} P^{\frac{1}{2}} = Y P^{-\frac{1}{2}}$$

$V_i, V_r$  = constants which can be physically interpreted as the incident and reflected waves at the terminals.

The relationship between the sending and receiving ends of a two-port network can be derived from equations A7.5 and A7.6 to give the well known admittance equation

$$\begin{bmatrix} I_S \\ I_R \end{bmatrix} = \begin{bmatrix} A & -B \\ -B & A \end{bmatrix} \cdot \begin{bmatrix} V_S \\ V_R \end{bmatrix} \quad (A7.7)$$

where

$$A = Y_0 \coth(P^{\frac{1}{2}} l)$$

$$B = Y_0 \operatorname{cosech}(P^{\frac{1}{2}} l)$$

$l$  = length of line considered

$I_S, I_R$  = sending end and receiving end currents

$V_S, V_R$  = sending end and receiving end voltages

Since  $P$  is non-diagonal, each of these equations represent  $n$  simultaneous differential equations and a direct solution of them is not self evident. This difficulty is overcome by making use of linear transform techniques.

If  $Q$  is the modal matrix of matrix  $P$ , and  $k$  is the eigen value matrix, then

$$P = Q k Q^{-1}$$

The propagation matrix  $\gamma$  is given by the expression

$$\gamma = k^{\frac{1}{2}}$$

and the characteristic admittance matrix  $Y_0$  by

$$\begin{aligned} Y_0 &= Y P^{-\frac{1}{2}} \\ &= Y Q \gamma^{-1} Q^{-1} \end{aligned}$$

On this basis, using properties of eigenvalues and eigenvectors, the two-port network parameters are given by the equation

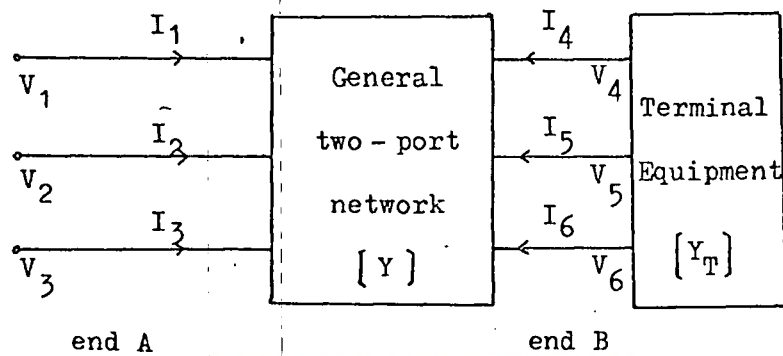
$$\begin{aligned} A &= Y_0 \text{Coth}(P^{\frac{1}{2}}l) = Y Q \gamma^{-1} \cdot \text{Coth} \gamma l \cdot Q^{-1} \\ B &= Y_0 \text{Cosech}(P^{\frac{1}{2}}l) = Y Q \gamma^{-1} \cdot \text{Cosech} \gamma l \cdot Q^{-1} \end{aligned}$$

The matrix functions  $\text{Coth} \gamma l$  and  $\text{Cosech} \gamma l$  are easily formed as they are diagonal matrices of elements  $\text{Coth} \gamma_i l$  and  $\text{Cosech} \gamma_i l$  respectively. Matrix multiplication then gives the two-port parameters. For both transmission lines as well as for cables, with assumptions of symmetry and zero voltage on earth conductors and sheaths the eigen-values and eigenvectors may be obtained in a straight forward manner, due to the properties the the symmetrical matrices. The series impedance and shunt admittance matrices are obtained as detailed in the former Appendices for the transmission line and cable.

## APPENDIX 8

REDUCTION OF A THREE-PHASE TWO-PORT NETWORK WITH KNOWN TERMINAL MATRIX  
TO OBTAIN EQUIVALENT ADMITTANCE MATRIX SEEN FROM INPUT END

In the method of analysis used in the present problem, it is quite often necessary to obtain the equivalent admittance matrix seen from the input end. The following section describes how this reduction is done.



University of Moratuwa, Sri Lanka  
 Electronic Theses & Dissertations  
 www.lib.moratuwa.ac.lk  
 Figure A 8.1

Figure A8.1 shows a general two-port network with admittance matrix  $[Y]$  and terminated by an admittance of  $[Y_T]$ . For the two-port network it is possible to write

$(6 \times 6)$   $(3 \times 3)$

$$\begin{bmatrix} I_1 \\ I_2 \\ I_3 \\ I_4 \\ I_5 \\ I_6 \end{bmatrix} = Y \begin{bmatrix} V_1 \\ V_2 \\ V_3 \\ V_4 \\ V_5 \\ V_6 \end{bmatrix} \quad (A8.1)$$



and for the terminal equipment it may be written that

$$\begin{bmatrix} I_4 \\ I_5 \\ I_6 \end{bmatrix} = - \begin{bmatrix} Y_T \end{bmatrix} \begin{bmatrix} V_4 \\ V_5 \\ V_6 \end{bmatrix} \quad (\text{A8.2})$$

combining equations A8.1 and A8.2 gives

$$\begin{bmatrix} I_1 \\ I_2 \\ I_3 \\ 0 \\ 0 \\ 0 \end{bmatrix} = \begin{bmatrix} [Y_{AA}] & [Y_{AB}] \\ [Y_{BA}] & [Y_{BB} + Y_T] \end{bmatrix} \begin{bmatrix} V_1 \\ V_2 \\ V_3 \\ V_4 \\ V_5 \\ V_6 \end{bmatrix} \quad (\text{A8.3})$$

where  $[Y_{AA}]$ ,  $[Y_{AB}]$ ,  $[Y_{BA}]$ , and  $[Y_{BB}]$  are the  $(3 \times 3)$  submatrices of the two-port network admittance matrix  $[Y]$ .

In compact notation, denoting input quantities by suffix A and output quantities with suffix B, we may write

$$\begin{bmatrix} \underline{I}_A \\ \underline{0} \end{bmatrix} = \begin{bmatrix} [Y_{AA}] & [Y_{AB}] \\ [Y_{BA}] & [Y_{BB}'] \end{bmatrix} \begin{bmatrix} \underline{V}_A \\ \underline{V}_B \end{bmatrix} \quad (\text{A8.4})$$

where  $[Y_{BB}'] = [Y_{BB}] + [Y_T]$ ,  $\underline{I}_B = -[Y_T] \cdot \underline{V}_B$

From equation A8.4,  $\underline{V}_B$  may be expressed in terms of  $\underline{V}_A$  as

$$\underline{0} = [Y_{BA}] \underline{V}_A + [Y_{BB}'] \underline{V}_B$$

$$\text{or} \quad \underline{V}_B = -[Y_{BB}']^{-1} [Y_{BA}] \underline{V}_A$$

Thus  $\underline{I}_A$  may be expressed in terms of  $\underline{V}_A$  as

$$\begin{aligned}\underline{I}_A &= \begin{bmatrix} Y_{AA} \end{bmatrix} \underline{V}_A - \begin{bmatrix} Y_{AB} \end{bmatrix} \begin{bmatrix} Y_{BB} \end{bmatrix}^{-1} \begin{bmatrix} Y_{BA} \end{bmatrix} \underline{V}_A \\ &= \left[ \begin{bmatrix} Y_{AA} \end{bmatrix} - \begin{bmatrix} Y_{AB} \end{bmatrix} \begin{bmatrix} Y_{BB} \end{bmatrix}^{-1} \begin{bmatrix} Y_{BA} \end{bmatrix} \right] \underline{V}_A\end{aligned}$$

In compact notation, this may be rewritten as

$$\underline{I}_A = \begin{bmatrix} Y_A \end{bmatrix} \underline{V}_A \quad (\text{A8.5})$$

where the equivalent admittance matrix seen from the input terminals is given by

$$\begin{bmatrix} Y_A \end{bmatrix} = \begin{bmatrix} Y_{AA} \end{bmatrix} - \begin{bmatrix} Y_{AB} \end{bmatrix} \begin{bmatrix} Y_{BB} + Y_T \end{bmatrix}^{-1} \begin{bmatrix} Y_{BA} \end{bmatrix} \quad (\text{A8.6})$$



APPENDIX 9

PIECEWISE FOURIER TRANSFORM OF FUNCTIONS AT REGULAR TIME INTERVALS

When sequential switching operations are investigated, the analysis for the closure of the second and third poles require the transform of certain voltages existing in the system prior to closure. These voltages are known at discrete time intervals, so that the transform needs to be obtained numerically. The following section<sup>31</sup> describes how this is obtained for the waveform shown in figure A9.1.

The transform of the piecewise function is obtained as the sum of the transforms of the  $(M - N)$  strips of width  $T_0$ . Consider a typical strip as shown in figure A9.2. If  $f_{k-1}$  and  $f_k$  are the values of the function at  $(k-1)T_0$  and  $kT_0$  respectively, then the Fourier transform of the function bounded by  $(k-1)T_0$ ,  $f_{k-1}$ ,  $f_k$  and  $kT_0$  can be found by decomposing the strip into a series of step and ramp functions whose transforms are readily obtained. A possible reduction for this chosen strip is also shown in figure A9.2, with two step and two ramp functions. The magnitudes of the steps are  $f_{k-1}$  and  $-f_k$ ; and the slopes of the ramp functions are  $\Delta f_k/T_0$  and  $-\Delta f_k/T_0$ .

The transform due to all the steps may be found by adding up the individual contributions. This is given by

$$f_s(\omega) = \frac{1}{j\omega} \left[ f_N \exp(-j\omega N T_0) - f_M \exp(-j\omega M T_0) \right]$$

Similarly, the Fourier transform of all the ramp functions can be found, and is given by

$$f_r(\omega) = -\frac{-1}{\omega^2 \cdot T_0} \sum_{k=N}^M (f_k - f_{k-1}) \cdot \left[ \exp(-j\omega(k-1)T_0) - \exp(-j\omega k T_0) \right]$$

The complete transform of the piecewise function  $f(t)$  is now given by

$$f(\omega) = f_s(\omega) + f_r(\omega)$$

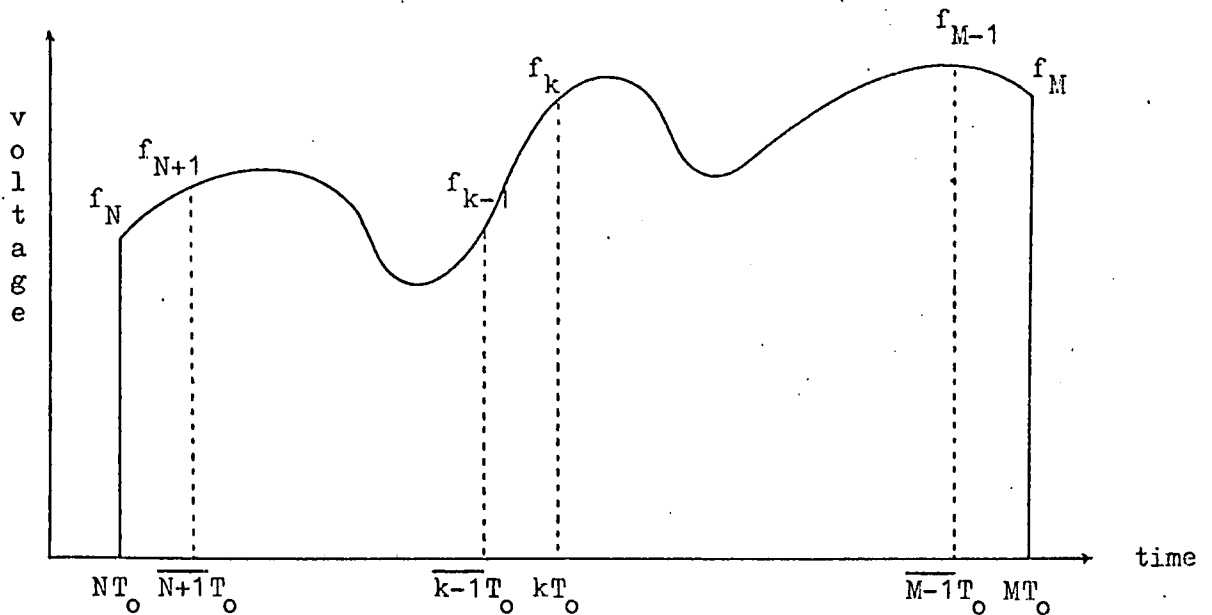


Figure A9.1 Waveform whose transform is required

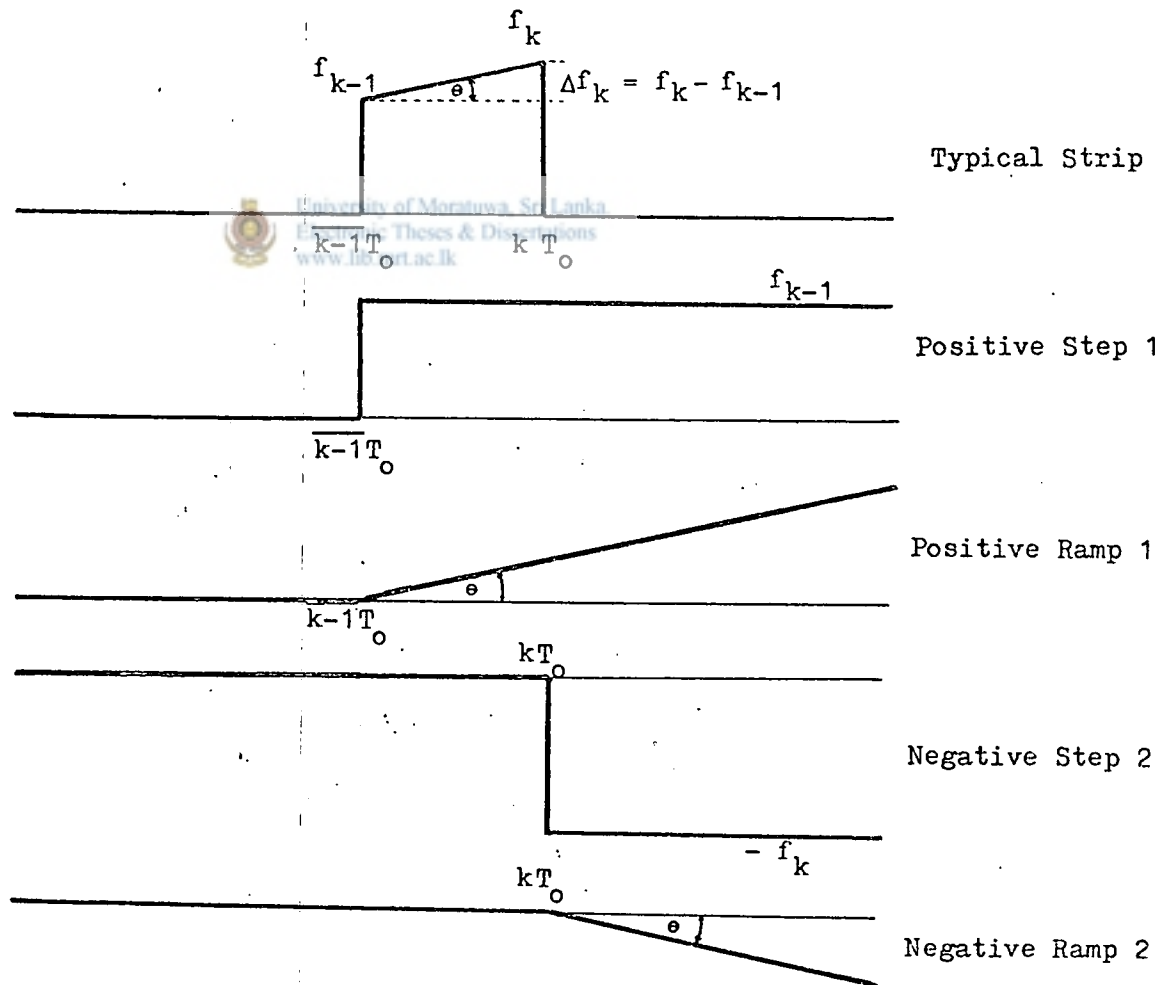


Figure A9.2 Synthesis of a typical strip of waveform

